day 12.5 (E12.5) [83]. However, at birth *Hox11* mutant limbs are dramatically shorter than controls and chondrocyte differentiation appears to have arrested at an early stage [83]. Histological examination of the skeletal elements at E18.5 reveals only small round immature chondrocytes with little or no sign of further chondrocyte differentiation [83]. On the medial anterior aspect of the radius there is typically a wedge shaped region of hypertrophic-like chondrocytes, but markers of mature hypertrophic chondrocyte matrix, like collagen X, are lacking [16, 83]. There is also no evidence of osteoblast differentiation in these mutants.

Several key signaling pathways are involved in establishing the spatially organized chondrogenic differentiation program within the developing skeletal element. *Indian Hedgehog* (*Ihh*), a ligand of the Hedgehog signaling pathway, and *Parathyroid hormone-related protein* (*PTHrP*) function in a paracrine fashion to regulate chondrocyte proliferation and the timing of hypertrophic differentiation [148]. *PTHrP* is expressed by perichondrial cells and early proliferative chondrocytes at the distal ends of the elements while the PTH receptor is expressed at low levels in proliferative chondrocytes and higher levels in prehypertrophic/hypertrophic chondrocytes [148]. PTHrP signaling functions to promote chondrocyte proliferation while inhibiting differentiation [188-191]. As chondrocytes become sufficiently distant from the source of *PTHrP*, proliferation stops and *Ihh* expression is initiated in prehypertrophic chondrocytes. Ligand is secreted by prehypertrophic chondrocytes and functions to promote chondrocyte proliferation and inhibit chondrocyte hypertrophy [192-195]. The pro-proliferative function of Ihh is thought to be through direct signaling to the chondrocytes themselves [196, 197]. Ihh-mediated inhibition of chondrocyte differentiation is accomplished indirectly through PTHrP. Ihh signals through the perichondrium, through an unknown mechanism, to promote *PTHrP* synthesis at the distal ends of the skeletal element [194, 195]. Together, the activities of Ihh and PTHrP regulate the timing of chondrocyte proliferation and differentiation.

Several other genes regulate the transitions between the different stages of chondrocyte differentiation. Runx2 regulates hypertrophic differentiation directly within chondrocytes themselves and indirectly within the perichondrium. During early skeletal development, *Runx2* is expressed transiently in proliferating chondrocytes at E12.5 and

appears to function in an Ihh-dependent manner to promote hypertrophy [198]. There is some evidence that Runx2 participates in the Ihh/PTHrP feedback loop. Runx2 binds to the *Ihh* promoter and directly promotes *Ihh* expression, while *Runx2* expression itself is inhibited by PTHrP [198, 199]. As development progresses, *Runx2* expression is downregulated in proliferative chondrocytes but remains high in prehypertrophic/hypertrophic chondrocytes and within the adjacent perichondrium. At later stages, Runx2 in the perichondrium appears to inhibit hypertrophy through the activity of FGF18 [200]. The Wnt ligands, *Wnt5a* and *Wnt5b*, are expressed in prehypertrophic chondrocytes and appear to regulate both the round to proliferative and the proliferative to hypertrophic transitions [201]. Unlike Runx2, these ligands appear to function in an Ihh-independent manner [201].

At first glance, the loss-of-function phenotypes of *Hox11*, *Ihh*, *Runx2*, and *Wnt5a* are remarkably similar characterized by significantly shortened skeletal elements and inappropriate chondrocyte differentiation [16, 194, 198, 201]. Closer examination on when and how chondrocyte differentiation is disrupted provides insight into a potential hierarchy in function of these genes. *Wnt5a* mutants have the mildest phenotype of all the mutants as despite the dramatic reduction in length, the general organization of the different zones of chondrogenic differentiation are preserved [201]. The zones of chondrogenic differentiation are completely disrupted in *Ihh* mutants which instead display a disorganized core of hypertrophic chondrocytes within the elements [194]. Runx2 and the closely related transcription factor Runx3 have redundant functions in skeletal development [198]. *Runx2/Runx3* double mutants display a complete blockade of chondrocyte development with the entire element consisting of small round chondrocytes [198]. With respect to all three of these genes, *Ihh*, *Runx2* and *Wnt5a*, loss of any one gene results in significant reduction or complete absence in the expression of the others, suggesting the regulation of these genes is intimately associated [194, 198, 201]. The similarity of the *Hox11* mutant phenotype to these mutants suggests potential interactions between Hox and Ihh, Runx2, or Wnt5a.

We provide data investigating the earliest stages skeletal development in control and *Hox11* mutant embryos to elucidate the initial defects observed in these mutants. Our preliminary studies strongly suggest an interaction between Hox11 and the Hedgehog

signaling pathway. These studies aimed to provide a framework for understanding the mechanisms for Hox function in early skeletal development.

Results

***Ihh*, *Runx2*, and *Wnt5a* expression are reduced in Hox11 mutants**

Skeletal preparations were performed on control, *Hox11* mutant (*Hoxa11-/-;Hoxd11-/-*), *Ihh* mutant (*Ihh-/-*), and *Wnt5a* mutant (*Wnt5a-/-*) forelimbs of embryos at E18.5 to specifically compare the zeugopod phenotype. Forelimbs were used for all of these studies to simplify the genetics of the *Hox11* mutants used. *Hoxa11* and *Hoxd11* are expressed in both the forelimb and hindlimb while *Hoxc11* expression is restricted to the hindlimb [16, 21]. Therefore, complete *Hox11* loss-of-function in the forelimb only requires loss of *Hoxa11* and *Hoxd11*, and these animals can be generated by conventional breeding techniques.

First, we performed skeletal preparations on the forelimbs of *Hox11* mutant (*Hox11aadd*), *Ihh* mutant, and *Wnt5a* mutant embryos at E18.5 to compare the morphology of the skeletal elements. Comparative analyses were restricted to the zeugopod elements, as the *Hox11* phenotype is restricted to this region of the limb. Compared to control forelimbs, the zeugopod bones in all three mutants are dramatically reduced in length, however there are subtle differences between the mutant phenotypes [Figure 4.1A]. *Hox11* mutant zeugopod bones are composed nearly completely of cartilage, indicated by the Alcian Blue staining, with a small calcified region on the anterior aspect of the radius, indicated by the Alizarin Red staining [Figure 4.1A]. The radius of the *Ihh* mutant is completely cartilaginous, while the ulna exhibits a disorganized core of calcified condensation [Figure 4.1A]. While *Wnt5a* mutant elements are reduced in size, the overall organization of the bones is somewhat preserved. The ulna displays cartilaginous regions at the distal ends of the bone with a medial ossified region, while the radius is completely composed of cartilage [Figure 4.1A].

We next compared the expression pattern of *Hox11*, using a Hoxa11eGFP knock-in reporter, to the expression of *Ihh*, *Runx2*, and *Wnt5a* detected by *in situ* hybridization at E12.5. The *Hoxa11eGFP* allele is a targeted knock-in/knock-out of eGFP to the endogenous *Hoxa11* locus [81]. Control animals are therefore heterozygous for *Hoxa11*, containing one *Hoxa11eGFP* allele (*Hox11AaG*), but wild-type for Hoxd11 (*Hox11DD*). As we have previously reported, Hoxa11eGFP expression is restricted to the stromal
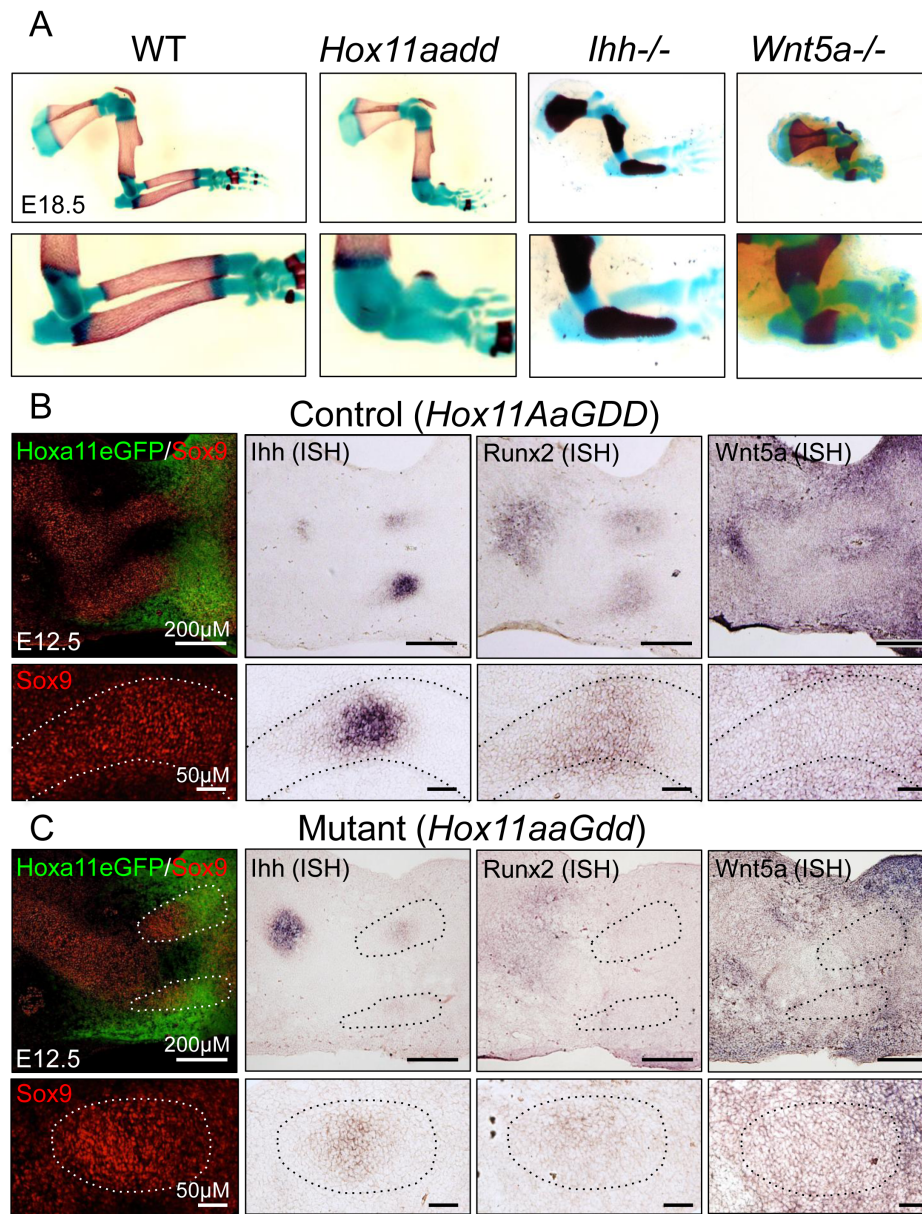
Figure 4.1: *Hox11*, *Ihh*, and *Wnt5a* **mutants have similar skeletal phenotypes; expression of** *Ihh*, *Runx2*, **and** *Wnt5a* **is reduced or absent at E12.5 in** *Hox11* **mutants.** (**A**) Forelimb skeletal preparations from control, *Hox11* mutant (*Hox11aadd*), *Ihh* mutant, and *Wnt5a* mutant at E18.5. Higher magnification images focus on the zeugopod (radius/ulna) elements and highlight striking similarities in the mutant phenotypes. (**B-C**) Adjacent longitudinal sections of E12.5 control (**B**) and *Hox11* mutant (**C**) forelimb zeugopod showing Sox9+ chondrocytes (red) and Hoxa11eGFP expression (green) by immunofluorescence and *Ihh*, *Runx2*, and *Wnt5a* expression by *in situ* hybridization (purple). High magnification images focus on the medial ulna. Dashed white lines on fluorescent images and dashed black lines on bright field images indicates boundary of skeletal elements determined by morphology and/or Sox9 expression.

connective tissue surrounding the zeugopod skeletal elements that are marked by Sox9 expression [Figure 4.1B]. Hoxa11eGFP in the perichondrium does not overlap with *Ihh* or *Runx2* expression, which are both expressed within Sox9+ chondrocytes at the medial region of the element [Figure 4.1B]. Higher magnification images show overlap of *Ihh* and *Runx2* within the chondrocytes [Figure 4.1B] Interestingly, there appears to be a layer of Sox9+ chondrocytes at the lateral sides of the element that are *Runx2*+ but *Ihh*- [Figure 4.1B]. This *Ihh* negative region may indicate the future osteoblast-forming region of the perichondrium at E14.5. In contrast, *Wnt5a* appears to be excluded from the Sox9+ chondrocytes and instead overlaps with Hoxa11eGFP in the perichondrium [Figure 4.1B].

The expression of all three of these genes is highly reduced or absent in *Hox11* mutants. *Hox11* mutant animals contain one *Hoxa11* mutant allele and the *Hoxa11eGFP* allele (*Hox11aaG*) and are null for *Hoxd11* (*Hox11dd*). It is important to note that Hoxa11eGFP expression continues to be largely restricted to the stromal tissues surrounding the Sox9+ skeletal elements consistent with the wild-type expression pattern [Figure 4.1C]. Therefore, GFP expression can be used to identify the cell population normally expressing *Hox11*. Very low levels of *Ihh* expression can be observed in a largely normal pattern in *Hox11* mutant anlage [Figure 4.1C]. Runx2 expression is highly reduced and Wnt5a expression, specifically within the zeugopod perichondrial region, is absent [Figure 4.1C].

By E14.5, the pattern of *Ihh*, *Runx2*, and *Wnt5a* has achieved their stereotypical expression domains. *Ihh* and *Runx2* are both expressed within prehypertrophic chondrocytes within the growth plate with *Runx2* additionally expressed within the perichondrium adjacent to the hypertrophic region [Figure 4.2]. *Wnt5a* is more broadly expressed within the growth plate in both the proliferative and prehypertrophic chondrocytes and also within the perichondrium, again more broadly than *Runx2* [Figure 4.2]. Hoxa11eGFP continues to be expressed in mesenchymal stromal cells throughout the perichondrium surrounding the skeletal elements [Figure 4.2]. Consistent with data from E12.5, the expression of *Ihh*, *Runx2*, and *Wnt5a* is severely reduced or absent in *Hox11* mutants [Figure 4.2]. There is a small region of *Ihh* expression within the anterior aspect of the radius with corresponding low levels of *Runx2* in the overlaying
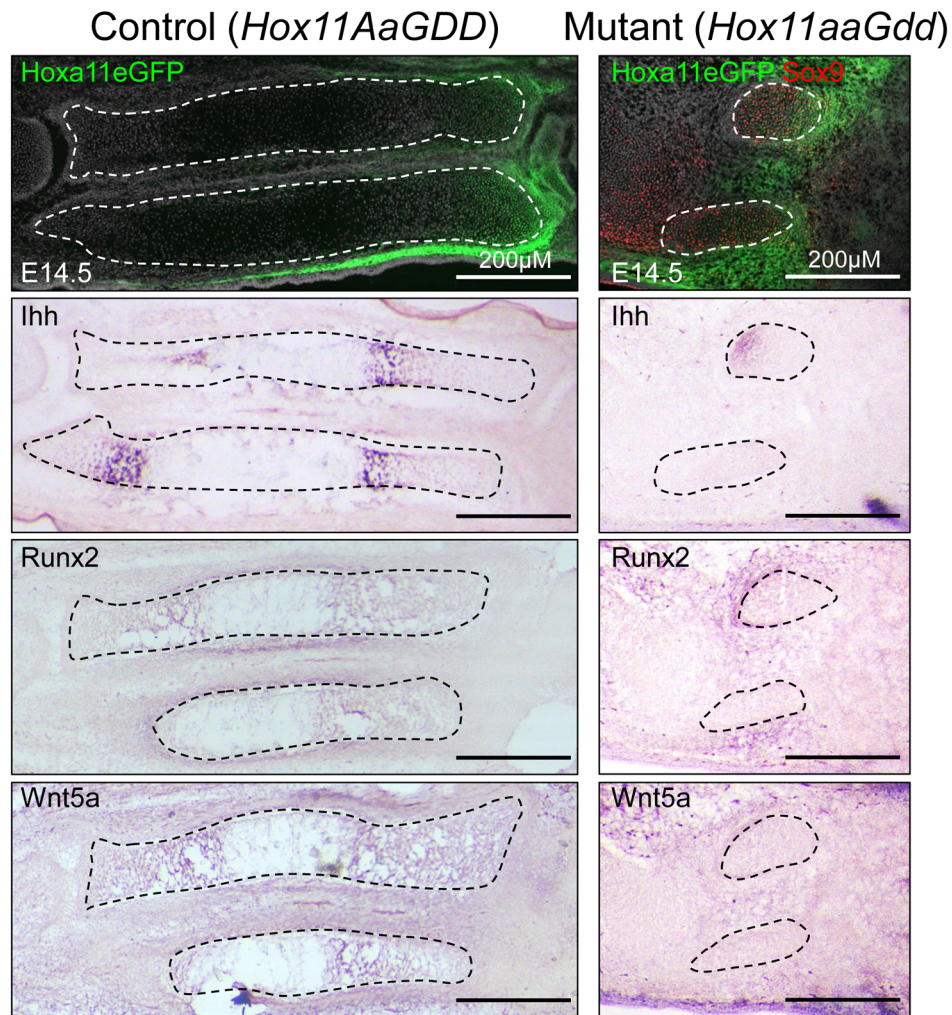
Figure 4.2: Expression of *Ihh*, *Runx2*, and *Wnt5a* is reduced in *Hox11* mutants at E14.5. Adjacent longitudinal sections of E14.5 control (left) and *Hox11* mutant (right) forelimb zeugopod showing Hoxa11eGFP expression (green) by immunofluorescence, and *Ihh*, *Runx2*, and *Wnt5a* expression by *in situ* hybridization (purple). Sox9+ chondrocytes (red) are marked in *Hox11* mutant to demarcate mis-patterned skeletal elements. Dashed white lines on fluorescent images and dashed black lines on bright field images indicates boundary of skeletal elements determined by morphology and/or Sox9 expression.

perichondrium that may correspond to the disorganized node of hypertrophic chondrocytes observed in *Hox11* mutants at E18.5 [Figure 4.1A, Figure 4.2].

Expression of *Ihh*, *Runx2*, and *Wnt5a* initiates concurrently at E12.5

To further understand the interaction hierarchy between *Hox11*, *Ihh*, *Runx2*, and *Wnt5a* in early skeletal development, the expression patterns of these genes were examined in the forelimbs of carefully staged embryos from E11.5 to E12.75. Hoxa11eGFP expression is first observed in the limb bud around E10.5 and becomes restricted to the developing zeugopod by E12.5 [Figure 4.3, [80]]. At E11.5, Sox9+ zeugopod pre-chondrocytes are beginning to condense in the zeugopod and Hoxa11eGFP expression is observed throughout the hand plate with the highest levels at the presumptive zeugopod boundary [Figure 4.3]. Zeugopod-specific expression of *Ihh*, *Runx2,* and *Wnt5a* is not yet observed [Figure 4.3]. At these stages, *Wnt5a* is expressed in a gradient within the handplate with the highest levels in the distal anterior ectodermal ridge and functions to promote limb bud outgrowth [202]. As Hoxa11eGFP expression becomes restricted to the zeugopod between E11.5 and E12.0, there continues to be no zeugopod specific expression of *Ihh*, *Runx2*, and *Wnt5a* [Figure 4.3]. Visible zeugopod specific expression of all of these genes is initiated at E12.5, in the previously described pattern, and continues thereafter [Figure 4.3]. These data define the transition between E11.5 and E12.5 as a critical time window for the early events that regulate organization of the skeletal elements.

Hox11-expressing cells are Hedgehog responsive

Ihh signals to the perichondrium as part of the PTHrP/Ihh feedback loop [194, 195]. The expression of Hoxa11eGFP within the perichondrial stromal cells suggested that Hox11-expressing cells may be responsive to Ihh signaling. LacZ reporter alleles for *Gli1-3* were used to identify Ihh responsive cells and to make predictions about Hedgehog activity within these cells. Gli1 is a transcriptional activator of the Hedgehog signaling pathway while also being a target of the pathway. Therefore activation of *Gli1*-lacZ expression and detection of β-gal activity by X-Gal staining can be used to identify cells within tissues that are actively responding to Hedgehog signaling [203]. At E12.5, *Gli1*-lacZ is observed at very high levels throughout the perichondrium and at lower
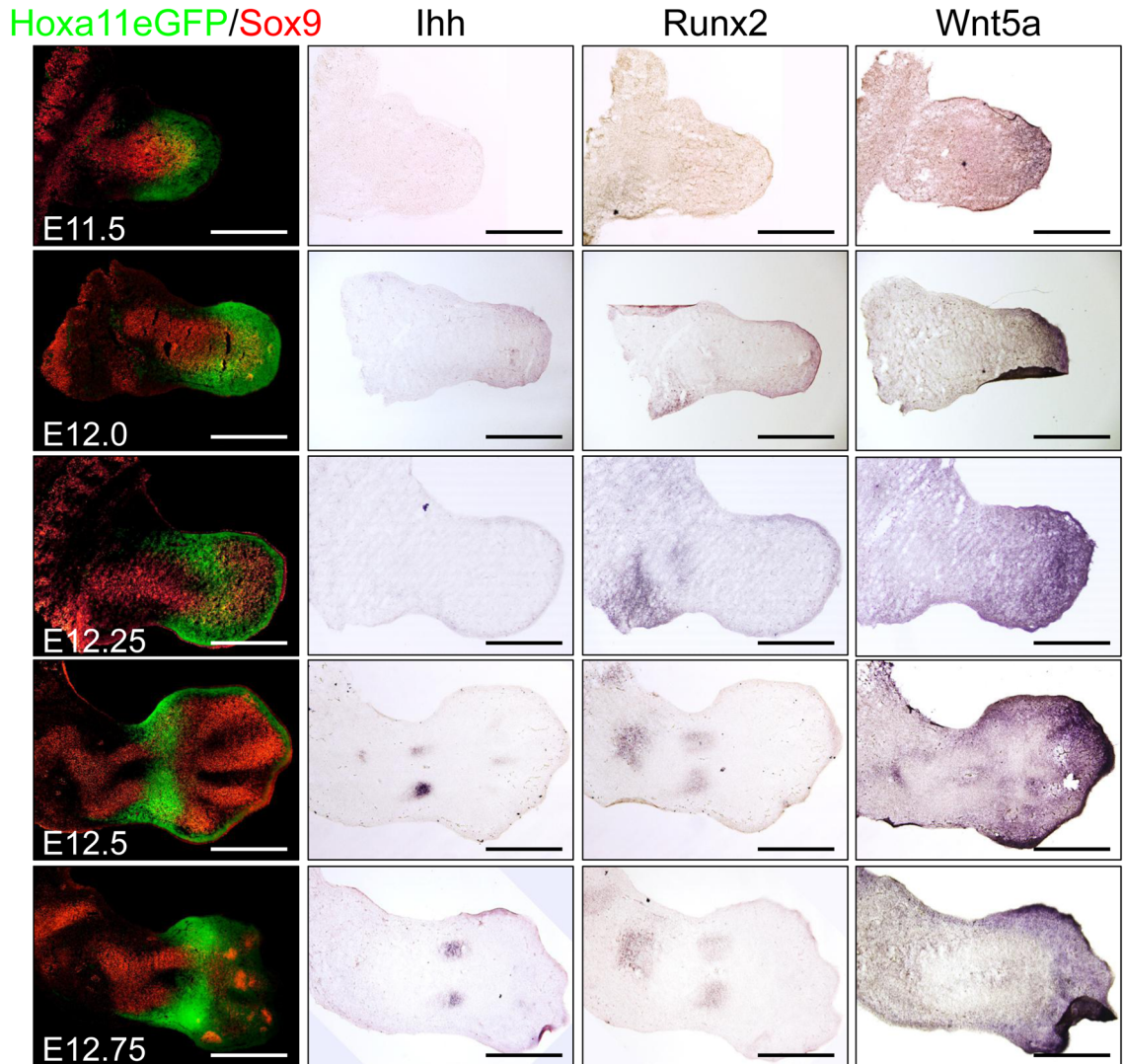
Figure 4.3: ***Ihh* and *Runx2* expression in the skeletal anlagen and perichondrial *Wnt5a* expression is initiated at E12.5**. Adjacent longitudinal sections of control forelimb zeugopod showing Sox9+ chondrocytes (red) and Hoxa11eGFP expression (green) by immunofluorescence and *Ihh*, *Runx2*, and *Wnt5a* expression by *in situ* hybridization (purple). Limb buds were staged based on morphology from E11.5 to E12.75. Scale bar = 500µm.

levels within the chondrocytes of the skeletal anlage [Figure 4.4A]. By E14.5, high levels of *Gli1*-lacZ continue to be observed throughout the perichondrium but LacZ is no longer detected within the element itself [Figure 4.4A]. In contrast, the bulk of *Gli2*-lacZ and *Gli3*-lacZ positive cells are restricted to the periarticular perichondrium at the distal ends of the skeletal elements [Figure 4.4A]. The perichondrial expression of all three Gli proteins overlaps with Hoxa11eGFP supporting the possibility that Hox11-expressing cells are Hh responsive [Figure 4.4A]. Interestingly, *Gli1*-lacZ is expressed in cells that lack *Gli2*-lacZ and *Gli3*-lacZ [Figure 4.4]. We next examined the pattern of *Gli1*-lacZ in Hox11 mutants at E12.5, E14.5, and E16.5. Consistent with the dramatic reduction in *Ihh* message, there is a significant reduction in *Gli1*-lacZ signal throughout the perichondrium in *Hox11* mutants [Figure 4.5]. This reduction in *Gli1*-lacZ is specific to the zeugopod region as wild-type levels are observed in the perichondrium of stylopod and autopod bones [Figure 4.5].

The location of *Ihh* expression, prehypertrophic chondrocytes, and the region of Hedgehog responsive cells in the perichondrium surrounding the entire element are spatially quite distant from one another [compare Figures 4.1B and 2 with Figure 4.4A]. It remains unclear if Ihh signal is propagated through the perichondrium or whether Ihh ligand functions as a long-range signal that acts directly on the distal perichondrial cells. The distribution of *Gli1*-lacZ signal in the perichondrium surrounding the entire element, including the most distal regions, provides evidence for the latter scenario. We investigated Ihh ligand distribution at E14.5 by immunohistochemistry using an antibody against the Hedgehog ligands. The highest level of ligand staining is observed at the boundary of the perichondrium and the underlying chondrocytes of the skeletal element [Figure 4.4B]. The levels are highest in the medial region of the element, near the site of ligand production, and decrease in a gradient fashion towards the distal ends of the elements. However, faint signal can still be observed even in the most distal regions [Figure 4.4B]. To validate the fidelity and specificity of the antibody, staining was performed in age matched *Ihh* mutant limbs. No specific staining within the skeletal elements was observed in *Ihh* mutant embryos, supporting the accuracy of our reported ligand distribution [Figure 4.4B].
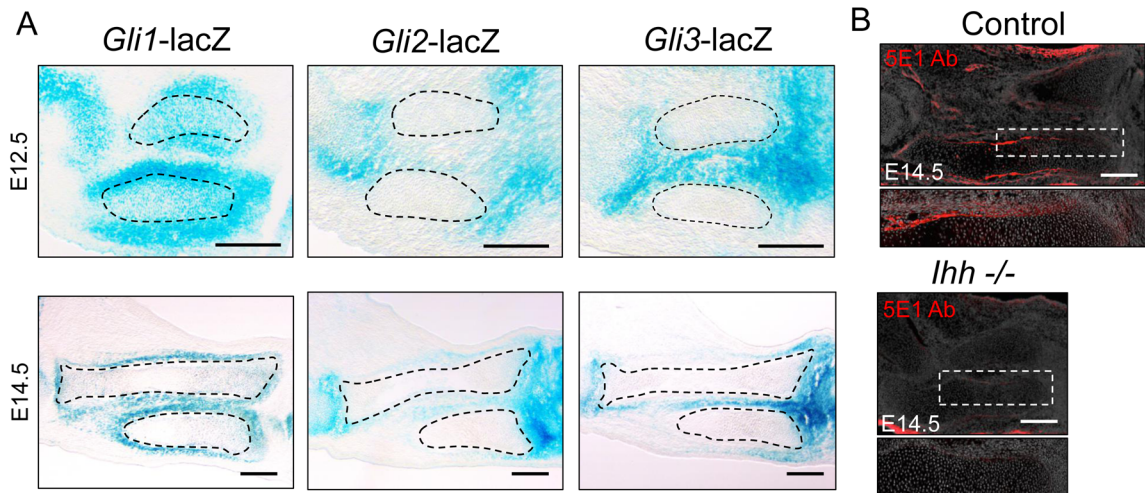
Figure 4.4: Hedgehog pathway responsive cells are generally restricted to the perichondrium and directly respond to Ihh ligand. (**A**) Longitudinal sections of E12.5 (top) and E14.5 (bottom) forelimb zeugopod from *Gli1*-lacZ, *Gli2*-lacZ, and *Gli3*-lacZ animals. β-galactosidase (blue) activity was detected by X-gal staining. Dashed black lines indicated boundary of skeletal elements determined by morphology. (**B**) Staining for Ihh protein (red) in E14.5 control or *Ihh* mutant (*Ihh-/-*) forelimb zeugopod using 5E1 antibody. Dashed white line indicates region magnified below. Scale bar = 200μm.
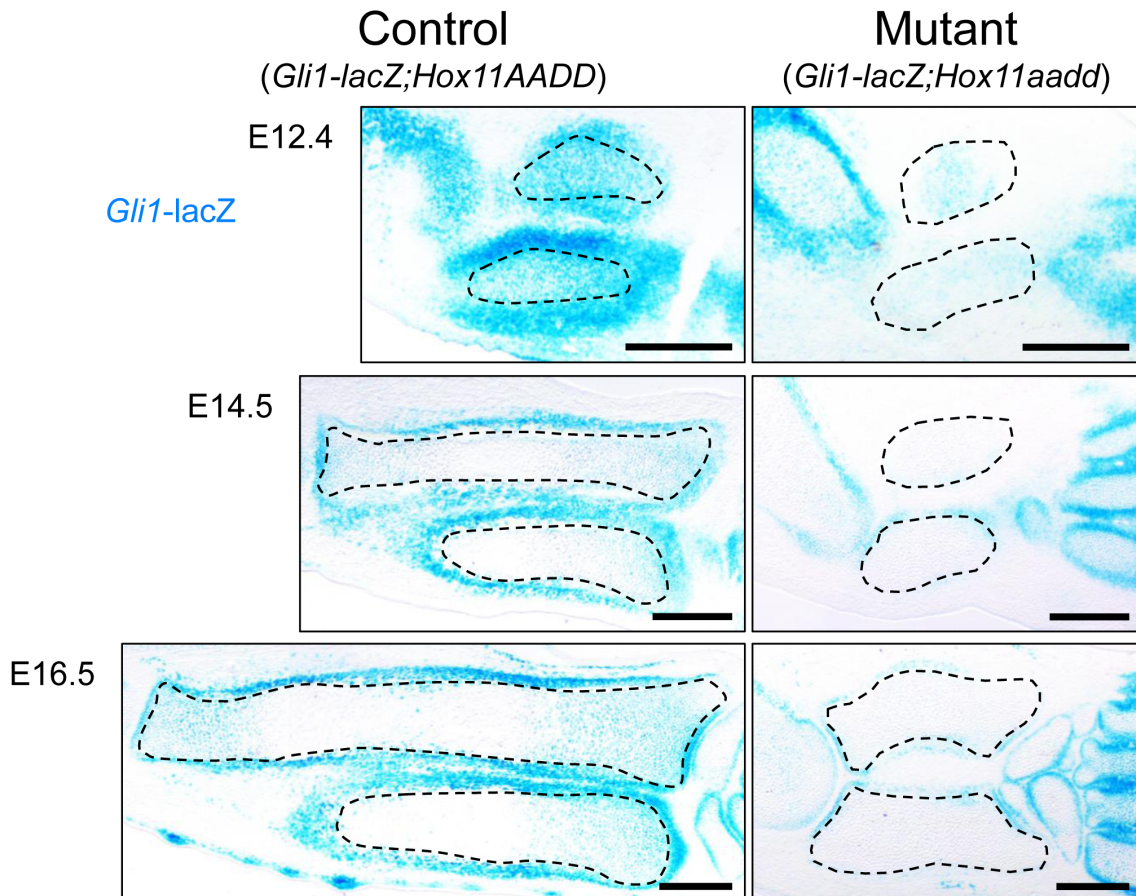
Figure 4.5: *Gli1*-lacZ signal is lost in *Hox11* mutant perichondrium. Longitudinal sections from E12.5, E14.5 and E16.5 control (left) and *Hox11* mutant (right) animals containing *Gli1*-lacZ allele. β-galactosidase (blue) activity was detected by X-gal staining Dashed black lines indicated boundary of skeletal elements determined by morphology. Scale bar = 500μm.

Hox11 mutants form cilia

The primary cilium is a non-motile, microtubule-based cell structure that projects from the cell surface that has reported functions as a signaling node for many pathways including Hedgehog signaling [reviewed [204]]. Many Hedgehog signaling components are specifically localized to the primary cilium, and disruptions in cilia formation or trafficking of intracellular components along the microtubules of the cilium correlates with Hedgehog signaling defects. We show that *Ihh* expression is, at least partially, initiated in *Hox11* mutant limbs at E12.5 yet there is little to no *Gli1*-lacZ response in the perichondrium suggesting that there is little to no Hedgehog pathway response. We hypothesized that *Hox11* mutants are unable to respond to Ihh ligand and, thus examined our *Hox11* mutant tissue for potential defects in the primary cilium.

The presence of cilia was examined at E12.5 and E14.5 in *Hox11* control and mutant forelimbs. At both stages examined, Hoxa11eGFP-positive perichondrial cells formed primary cilia that were indistinguishable from controls, although resolution in tissue is not high [Figure 4.6A-B]. To examine primary cilia at greater resolution, primary mouse embryonic fibroblast cultures were generated from *Hox11* control and mutant limb buds at E12.5 and the primary cilia was examined *in vitro*. Cilia formation appears normal in *Hox11* mutant fibroblast cultures compared to controls *in vitro*, as well [Figure 4.6C]. These data suggest that *Hox11* mutant cells form primary cilia and are likely to be capable of responding to Ihh ligand.

Next, we tested whether *Hox11* mutants were capable of responding to Hedgehog signaling by pharmacologically activating the pathway using Smoothened Agonist (SAG) in an *ex vivo* limb culture system [205]. This agent activates the Hedgehog signaling pathway at the level of the cell surface, bypassing Hedgehog ligand binding to the Patched-1 (Ptch1) receptor and directly activating Smoothened (Smo). For these experiments, *Hox11* control and mutant animals additionally contained *Gli1*-lacZ as a read out of Ihh pathway activation. Forelimb cultures were initiated at E12.5 and were treated with SAG or DMSO as a control. After 24 hours in culture, treatment with SAG rescued *Gli1*-lacZ signal in *Hox11* mutants to levels comparable to controls [Figure 4.7]. These data demonstrate that *Hox11* mutant cells are capable of responding to Hedgehog

signaling. However, after 72 hours in culture, SAG treatment did not lead to any phenotypic rescue of the *Hox11* mutant phenotype [data not shown]. It is still unclear whether the lack of phenotypic rescue is meaningful or simply due to limitations of the experimental conditions.
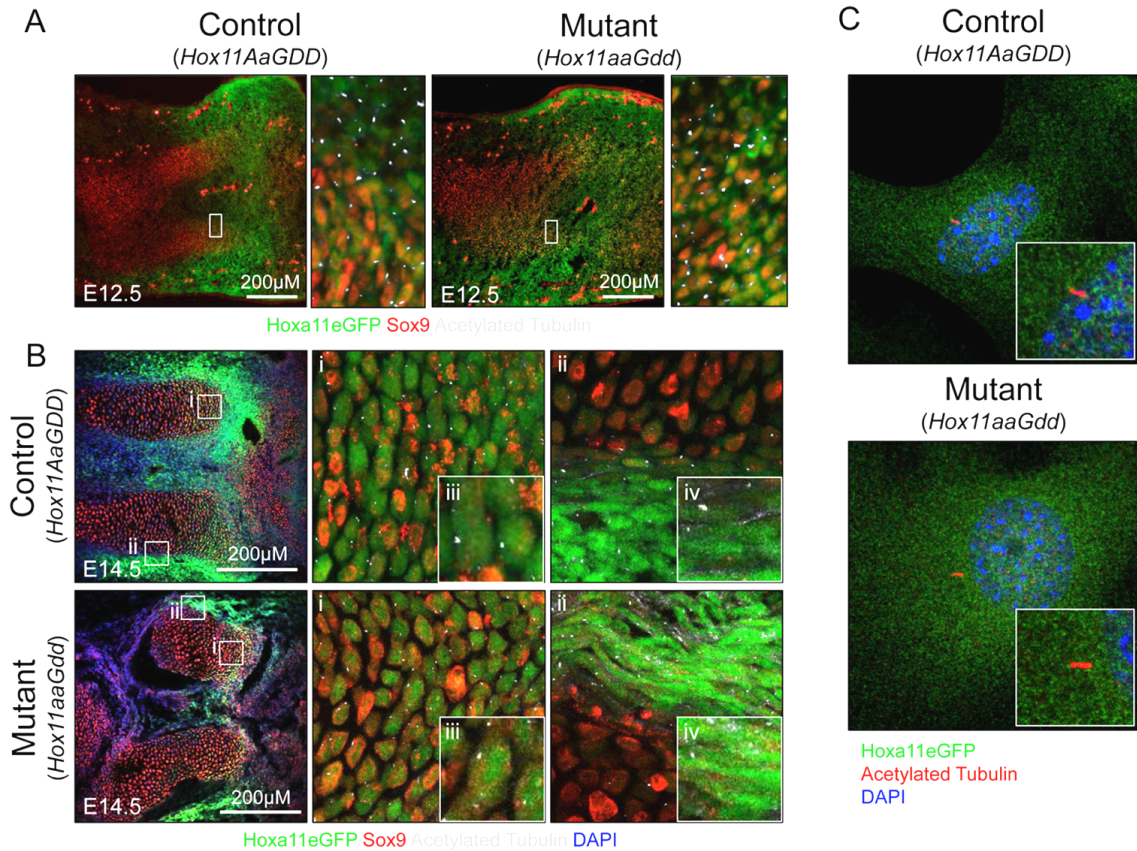
Figure 4.6: ***Hox11* mutants form primary cilia that are indistinguishable from controls**. Longitudinal section of zeugopod forelimb from control (left) and *Hox11* mutant (right) embryos containing *Hoxa11eGFP* allele (green) at E12.5 (**A**) or E14.5 (**B**). Sections were stained with Sox9 (red) to identify chondrogenic condensations and Acetylated Tubulin (white) to identify primary cilia. (**A**) White box indicates region magnified to right. (**B**) DAPI (blue) identifies all cell nuclei. White boxes (i and ii) indicate regions magnified to right of each low magnification image. Insets (iii and iv) are even higher magnification images of acetylated tubulin staining. (**C**) Primary limb bud fibroblasts isolated from E12.5 control (top) and *Hox11* mutant (bottom) embryos containing *Hoxa11eGFP* allele. Hoxa11eGFP-positive (green) cells were stained with Acetylated Tubulin (red) to identify primary cilia and DAPI (blue) to identify cell nuclei. Inset (white box) shows high magnification of primary cilia.
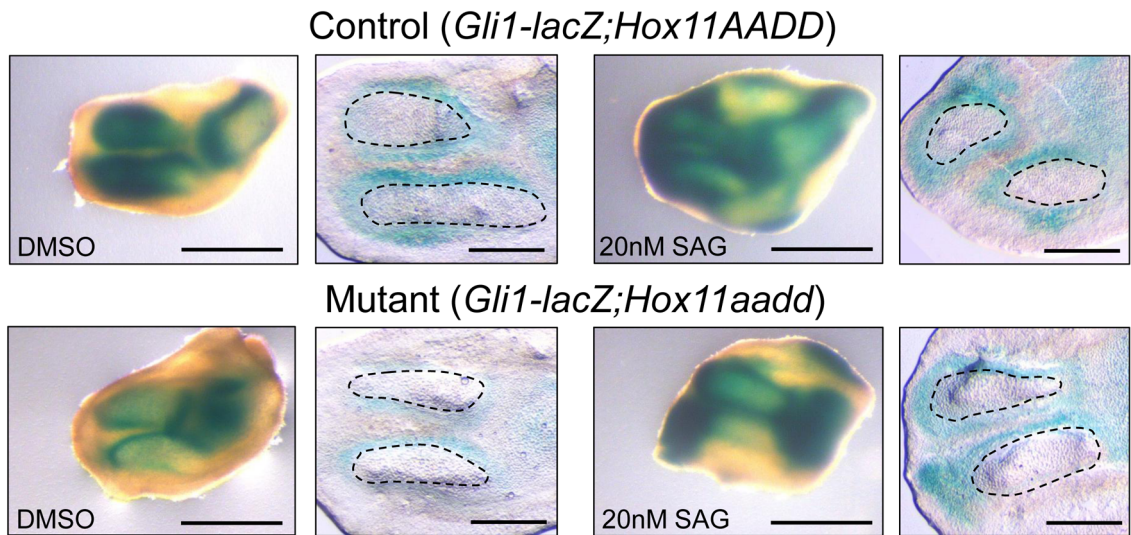
Figure 4.7: *Hox11* **mutant perichondrial cells are capable of responding to Hedgehog signaling in *ex vivo* culture when stimulated by Smoothened Agonist.** *Ex vivo* forelimb zeugopod cultures were established from control (top) and *Hox11* mutant (bottom) embryos that additionally contained the *Gli1*-lacZ allele. Forelimbs were cultured for 24 hours on membranes at the liquid-air interface prior to fixation and whole-mount X-gal staining (blue). The left forelimb culture media was supplemented with 20nM of Smoothened Agonist (SAG) while the right forelimb culture media contained vehicle control (DMSO). Whole-mount images were taken after staining (left panels). Limbs were subsequently embedded and sectioned and bright-field images collected (right panels). Dashed black lines indicated boundary of skeletal elements determined by morphology. Scale bar = 200μm.

Discussion

This work in progress aimed to characterize the earliest events in skeletal development in an effort to elucidate the mechanism of *Hox* function during these processes. Our initial hypothesis was if we could identify the earliest molecular event that is disrupted in *Hox11* mutant animals this would provide a clue as to the possible mechanism(s) of Hox-mediated patterning of the skeleton. We chose to characterize the expression profiles of *Ihh*, *Runx2*, and *Wnt5a* due to the striking similarities in the skeletal phenotypes of *Ihh*, *Runx/Runx3*, and *Wnt5a* mutants compared to the *Hox11* loss-of-function phenotype [16, 194, 198, 201]. We focused our analyses from E11.5 to E12.5 as this is when defects in *Hox11* mutants are first observed [83]. Our analyses showed that, within the level detection by *in situ* hybridization, expression of all three genes are initiated virtually concurrently at E12.5. These data define the E11.5 to E12.5 temporal window as a critical window for establishing many critical signaling events in skeletal development. Unfortunately, we were unable to determine an order in which these genes are expressed with the assays used. It is important to note that Hoxa11eGFP expression is observed days prior to the initiation of *Ihh*, *Runx2*, and *Wnt5a* expression suggesting Hox functions upstream of these genes and could be involved in initiating their expression.

At E12.5, Hoxa11eGFP-positive perichondrial cells are strongly *Gli1*-lacZ positive indicating that these cells actively respond to Ihh ligand. We did not examine *PTHrP* expression in this study, however prior studies indicate that *Hox11*-expression overlaps with *PTHrP* expression in perichondrial cells at the distal ends of the skeletal elements [83]. In addition to significant reduction in *Ihh* expression in *Hox11* mutants, *PTHrP* expression is also lost [83]. We have acquired a *PTHrP*-lacZ allele and future experiments will examine the levels of *PTHrP* expression in *Hox11* control and mutant embryos [206]. Perhaps unsurprisingly, with the dramatic reduction in *Ihh* expression in *Hox11* mutants there is a corresponding loss of *Gli1*-lacZ signal in the perichondrium and this loss of β-gal signal is specific to the zeugopod skeletal elements. These data strongly suggest a role for Hox11 in the negative feedback loop between Ihh and PTHrP. Specifically, it suggests that Hox11 may function to promote *PTHrP* expression in perichondrial cells in response to Ihh signaling. Given the significant physical distance

between the source of *Ihh* message and Hedgehog responsive cells, indicated by *Gli1*-lacZ, we investigated the distribution of Ihh protein within the skeletal elements. Our data indicate that Ihh ligand traverses from the site of production to the perichondrium, where it localizes and signals directly to the Hox11-expressing perichondrial cells.

There is precedence for long-range movement of Hedgehog ligands distant from the location of ligand secretion [207, 208]. Diffusion of Hedgehog ligands appears to depend significantly on the composition of the extracellular matrix particularly heparan sulfate proteoglycans [207, 208]. Changes in the heparan sulfate chains can dramatically affect Hedgehog ligand distribution. In the skeleton, mutants of the glycosyltransferase Exostosin 1 (Ext1) have reduced heparan sulfate synthesis and exhibit an increased range of Ihh ligand distribution, specifically within the growth plate [208]. Koziel and colleagues report Ihh ligand distribution in a gradient within the chondrocyte extracellular matrix of the growth plate with the highest levels corresponding to pre-hypertrophic zone and the source of *Ihh* transcription [208]. Expression within the perichondrium was not reported in this study, but levels appear to be low or absent. The distribution of Ihh ligand reported in this study is not consistent with the pattern of distribution we report. The 5E1 antibody used in our work is a mouse primary antibody and results in high background signal within the tissue, overall increasing the technical difficulties involved for these experiments. However, we used littermate *Ihh*$^{-/-}$ controls as our negative control for these studies, increasing our confidence in the accuracy of the staining pattern we report. It is possible that further optimization of the antibody staining protocol could allow us to visualize Ihh ligand within the growth plate as well as the perichondrium, potentially resolving the discrepancy in the pattern of ligand distribution.

We show that at E12.5 there is a small amount of *Ihh* message generated in *Hox11* mutant skeletal elements but this is lost by E14.5. These data suggest that initiation of *Ihh* expression in the skeletal anlage is Hox-independent but that maintenance of this expression is Hox-dependent. This might be expected as Ihh expression initiates in non-Hox-expressing cells. Additionally, there is no *Gli1*-lacZ signal in the perichondrium of *Hox11* mutants indicating no Hedgehog pathway activation. We hypothesized that *Hox11* mutant perichondrial cells may be unable to respond to Ihh signaling resulting in a failure to establish appropriate feedback signaling required to maintain *Ihh* expression. However,

analysis of cilia formation demonstrated that *Hox11* mutant perichondrial cells were capable of forming normal cilia suggesting that *Hox11* mutants should be capable of responding to Ihh ligand at the cell surface. A caveat to this conclusion is the current level of analyses is not at very high resolution and further study would allow this conclusion to be more highly supported. Additionally, pharmacologic activation of Hedgehog signaling with SAG in *ex vivo* limb cultures confirmed that *Hox11* mutants were able to respond to Hedgehog signaling indicated by a rescue of *Gli1*-lacZ expression in the perichondrium. SAG activates the Hedgehog signaling pathway at the level of the cell surface through direct activation of Smoothened. In Hedgehog signaling, Ptch1 inhibition of Smo activity is released upon ligand binding initiating downstream signaling cascade resulting in expression of Hedgehog target genes, like Gli1 [209]. Gli1 is both a target and an effecter of Hedgehog signaling. Our *ex vivo* culture analyses allow us to conclude that, from the level of Smo, activation of Hedgehog signaling is capable of upregulating, at least some, downstream targets in *Hox11* mutants. However, activation of Hedgehog signaling was unable to morphologically rescue the *Hox11* mutant phenotype suggesting activation of a subset of downstream Ihh targets in the perichondrium may still be defective even though *Gli1* expression is induced. These data are consistent with the exciting possibility that Hox11 and Gli1 transcription factors may work cooperatively within the perichondrium.

Future Directions

Short-term experiments

This study provides the foundation for future work in understanding the earliest events regulated by Hox11 during skeletal development and focuses future analyses to the E11.5 to E12.5 temporal window. The earliest phenotypic changes in *Hox11* mutants occurs beginning at E12.5, the time point when multiple known signaling molecules and transcription factors critical for proper skeletal development are first being expressed. Given that expression of *Ihh*, *Runx2* and *Wnt5a* are all reduced or absent at E12.5 in *Hox11* mutants, these data suggest early functions for Hox11 in regulating these genes. However, only Wnt5a expression overlaps with Hoxa11eGFP in the perichondrium indicating that Hox11 does not directly regulate the expression of *Ihh* or *Runx2,* but may regulate *Wnt5a* expression. Additionally, initiation of *Ihh* expression appears to be Hox-independent at E12.5 indicating Hox11 may function within the Ihh/PTHrP feedback loop downstream of Ihh signaling, perhaps through direct interactions with Gli transcription factors.

Recent data has provided insight into the mechanisms that control initiation of *Runx2* and *Ihh* expression within the skeletal anlagen. Runx2 has previously been shown to directly activate *Ihh* transcription within chondrocytes [198]. New evidence suggests redundant functions of perichondrial FGF9 and FGF18 in promoting both *Runx2* and *Ihh* expression during early limb development [210]. The authors propose a model whereby FGF9 and FGF18 regulate early chondrocyte proliferation through initiating the Ihh/PTHrP feedback loop. *FGF9* and *FGF18* are both expressed within the limb bud mesenchyme and the perichondrium at early stages of skeletal developing suggesting that these genes could potentially be directly regulated by Hox11. It is important to note, however, that the *Fgf9;Fgf18* double mutant phenotype most severely affects the stylopod bones suggesting redundant functions for other FGFs within the zeugopod [210]. Future experiments will examine expression of *Fgf9* and *Fgf18* in *Hox11* control and mutant embryos by *in situ* hybridization between E11.5 and E14.5. Additionally, we have recently acquired an *Fgf18*-lacZ reporter allele that can be used as a secondary means of examining FGF18 expression [gift from Dr. Mark Lewandoski]. The

relationship between Hox11 and FGF ligands in the limb could provide a mechanism for Hox11 regulation of Runx2 and Ihh expression in early skeletal development. However, the *Hox11* mutant phenotype is significantly more severe than the *Fgf9;Fgf18* double mutant indicating additional functions beyond potentially regulating FGF ligands.

Our preliminary data supports multiple interactions between Hox11 and Ihh signaling. First, Ihh expression is lost in *Hox11* mutants indicating that Hox11 functions early during development to indirectly promote Ihh expression. Second, *Gli1*-lacZ staining indicates that Hox11-expressing cells respond to Ihh signaling throughout skeletal development. We present preliminary evidence that primary cilia formation occurs normally in *Hox11* mutants indicating that these cells should be capable of responding to Hedgehog ligands at the cell surface. However, the current data from limb tissues is purely qualitative and cilia resolution is not high enough for quantification of properties like cilia length. Data from *Hox11* control and mutant limb bud fibroblasts provides additional qualitative evidence supporting normal cilia formation in mutants. However, cilia morphology was assessed in limb bud fibroblasts that had been maintained in culture for multiple passages (>5) raising concerns about the effects of *in vitro* culture on cell behavior. Future studies quantifying cilia length using primary limb bud fibroblast cultures at early passage numbers (<2) will provide the rigor necessary to identify potential cilia defects. If differences in cilia length are observed, ultra-high resolution techniques, like electron microcopy, could be used to examine the microtubular structure of the cilia.

Consistent with our preliminary data indicating normal cilia formation, e*x vivo* limb cultures strongly support that *Hox11*-mutant perichondrial cells are capable of responding to Hedgehog signaling, at least to the extent of activation of the downstream Hedgehog target gene, *Gli1*. Treatment with SAG was unable to affect any phenotypic rescue of the *Hox11* mutant skeleton at any concentration tested, and at all but the lowest concentrations (<10μM), had a negative effect on development of wild-type limb cultures [data not shown]. It is still unclear whether the lack of a rescue is a meaningful result or simply a consequence of the experimental conditions. However, it is important to note that SAG treatment, at the concentrations tested was unable to rescue *Ihh* mutant limb development either indicating critical experimental design problems [data not shown].

SAG is a powerful activator of the Hedgehog pathway and skeletal development may be very sensitive to the degree of Hedgehog pathway activation. Future rescue experiment using purified Ihh ligand may yield more informative results. Full or partial rescue of the *Ihh* mutant phenotype is a critical control that must be accomplished prior to further *ex vivo* attempts at rescuing *Hox11* mutants. Access to *Wnt5a* mutants provides an additional opportunity to attempt to rescue the *Hox11* mutant phenotype through supplementation of exogenous Wnt5a ligand. Appropriate control experiments to rescue the *Wnt5a* mutant phenotype have not been performed, however exogenous Wnt5a ligand resulted in a mild increase in chondrocyte proliferation in *Hox11* mutants but no rescue of chondrocyte morphology [data not shown]. Defects in FGF signaling in *Hox11* mutants has yet to be determined, but exogenous FGF9 and/or FGF18 represent additional candidates for *ex vivo* rescue. It is possible that an *ex vivo* rescue will not be successful due to the complex signaling interactions between multiple pathways and more complex genetic rescues could be considered.

Long-term experiments

In general, the proposed experiments still fall short of understanding the direct molecular mechanisms of *Hox11* function in skeletal development. *Hox* function appears to be critical for initiating multiple signaling pathways involved in the initial stages of skeletal development between E11.5 and E12.5, a temporal window that has been significantly understudied. There is a clear relationship between Runx2 and Ihh signaling, potentially involving FGF9/FGF18, but the function of *Hox* within these interactions is unknown. Additionally, the function of Wnt5a produced in the perichondrium has not been explored. Hypothesis generating assays, like chromatin immunoprecipitation (ChIP), microarray, or RNA sequencing (RNAseq), will be necessary to identify mechanisms of Hox function at these developmental stages. We have previously performed microarray analyses at E12.5 comparing the expression profile of Hoxa11eGFP-expressing control and mutant limb bud stromal cells. The top Gene Ontology (GO) term from these data was genes related the extracellular matrix suggesting Hox may function in regulating the extracellular environment during early development. Disappointingly, the fold-changes of most of these genes were less than two-fold making it difficult to confidently validate potential target genes by qPCR or *in*

situ hybridization. Future experiments may involve comparing expression changes in controls and mutants over multiple time points as our prior experiments may not have captured the most informative snapshot.

For some of these data-generating experiments, new mouse models will be required to perform *in vivo.* Efforts are currently underway to generate knock-in FLAG-tagged versions of *Hoxa11* and *Hoxd11* to allow us to perform pull down experiments on these proteins. Available antibodies are not specific or sensitive enough for individual Hox proteins to allow for assays like ChIP or co-immunoprecipitation (Co-IP) on endogenous Hox protein. Generation of knock-in tagged alleles will allow us to circumvent limitations in anti-Hox antibody quality by isolating Hox proteins by their tags, in this case FLAG. Importantly, this targeted knock-in approach maintains Hox expression at endogenous levels minimizing concerns about false positives due to over expression of your gene of interest. ChIP experiments will allow us to identify genes, at the whole genome level, that may be regulated by Hox11 at these stages. Candidate genes can then be validated *in vivo*. We can also use a targeted approach to look for Hox11 binding near candidate genes from our microarray or other assays. FLAG-tagged alleles will also allow us to perform Co-IP experiments to test our hypothesis that Hox11 and Gli1 directly interact to promote downstream Hedgehog signaling. A Hox11 binding-partner screen could even be performed using Co-IP followed by mass-spectrometry of isolated proteins. Collectively these experiments have significant potential to increase our understanding of the mechanisms of Hox gene function in skeletal development.

Other studies presented in this thesis identified Hox11-expressing stromal cells as a life-long skeletal stem cell that arises at embryonic stages [Pineault *et al. in submission*]. Prior work established that *Hox11* is not required for MSC specification during development but that loss of Hox11 function resulted in chondrogenic and osteogenic differentiation defects *in vivo* [110]. These data suggest Hox11 may function in early fate decisions in skeletal MSCs. Chondrogenic progenitors for the forelimb zeugopod express the transcription factor *Sox9* and generate a Collagen II matrix, both indications of early chondrocyte lineage specification seemingly inconsistent with our hypothesis [83]. However, initiation of *Sox9* expression occurs prior to overt regional restriction of the posterior *Hox* genes (*Hox9-13*) within the limb bud. During these initial

skeletal condensation events, there is significant overlap in expression of the posterior Hox genes and redundancy between the Hox paralogous groups may be sufficient to compensate for loss of *Hox11* genes at this stage. As limb development proceeds, posterior Hox gene expression and function is regionally restricted, and potential compensation is lost. The initial manifestation of *Hox11* mutant phenotypes at E12.5 coincides nicely with the restriction of Hoxa11eGFP expression to the zeugopod supporting this hypothesis [80, 83]. Thus, the failure of the zeugopod elements to undergo subsequent longitudinal growth following element condensation may result from a failure of *Hox11* mutant skeletal MSCs to undergo chondrogenic differentiation and contribute new skeletal cells. One potential experiment to address the function of Hox11 in early fate decisions is through careful molecular analyses of directed chondrogenic differentiation of Hox11-expressing skeletal progenitors *in vitro*. RNA sequencing (RNAseq) could be performed at multiple points during the early stages of directed differentiation to analyze the transcriptome of cells differentiated from *Hox11* control and *Hox11* mutant progenitors. These studies could allow for identification of candidate genes involved in the early chondrogenic program that are regulated by Hox11 that could subsequently be confirmed *in vivo*.

Materials and Methods

Mouse models

All animals were maintained on mixed backgrounds. *Hoxa11eGFP* [81], *Ihh*-mutant [194], *Wnt5a*-mutant [202], *Gli1*-lacZ [203], *Gli2*-lacZ [211], *Gli3*-lacZ [212], and *Hoxa11* and *Hoxd11* null alleles [83] have been described elsewhere. Control and Hox11 null embryos were generated by crossing double heterozygous parents of the following genotypes; *Hox11AaGDd* x *Hox11AaDd*. Mating pairs were checked daily for the presence of a vaginal plug. Pregnant females were sacrificed by CO2 exposure at the indicated ages. All procedures described here were conducted in compliance with the University of Michigan Committee of Use and Care of Animals, protocol PRO00006651.

Skeletal preparations

E18.5 embryos were eviscerated and fixed in 95% ethanol overnight. Skeletal preparations were performed using standard methods [213].

In situ hybridization and immunohistochemistry

Embryos were collected in PBS on ice, fixed in 4% parafolmaldehyde for 2 hours at 4 C rocking, and equilibrated in 30% sucrose overnight. Tissues were embedded in optical cutting temperature (OCT) medium and sectioned at 12μm. Section *in situ* hybridization was performed as previously described [214, 215]. *Ihh, Runx2*, and *Wnt5a in situ* probes were previously described [192, 216, 217]. Section immunohistochemistry was performed using standard methods using primary antibody for rabbit anti-Sox 9 (1:500, Millipore, AB5535) and conjugated secondary antibodies donkey anti-rabbit Alexa Fluor 555 (1:1000, Invitrogen, A31572). Mouse on Mouse detection kit (Vector Labs) was used to detect mouse anti-acetylated Tubulin (1:20, Sigma, T7451) and mouse anti-Shh/Ihh (Developmental Studies Hybridoma bank, 5E1) using M.O.M. Biotinylated Anti-Mouse IgG reagent and Streptavidin Alexa Fluor 647 (1:500, BioLegend, 405237). β-Galactosidase staining was performed as described (Mortlock 2003). Nuclei were visualized by DAPI (1:10,000, Sigma, D9542). Fluorescent and bright-field images were captured on an Olympus BX-51 microscope with an Olympus DP-70 camera.

Cell culture

Mouse limb bud fibroblasts were harvested from E12.5 forelimbs from control and *Hox11* mutant *Hoxa11eGFP*-positive embryos. Embryos were harvested in sterile PBS on ice. Using a stereo microscope equipped with a fluorescence adaptor, only the Hoxa11eGFP-positive region of the forelimb was harvested. Forelimb tissue was rinsed several times in sterile PBS. Tissue was digested with 0.25% Trypsin-EDTA (Gibco) at 37 C with mild agitation for up to 5 minutes. Digestion reaction was quenched with culture media (Dulbecco's Modefied Eagle's Media (DMEM) containing 10% FBS, 1% L-glutamine, 1% Penicillin and Streptomycin). A single cell suspension was generated by repeated, gentle agitation with a p1000 pipette. Tissue-culture dishes were coated with 0.1% gelatin prior to limb fibroblast culture. Fibroblasts from a single embryo were plated onto one well of a 6-well plate and culture media was changed every other day. Cells were passaged upon reaching 70-80% confluence using standard Trypsin methods.

For imaging, cells were cultured on gelatin coated glass coverslips until reaching 70-80% confluence. Cells were rinsed with ice-cold PBS and fixed with 4% paraformaldehyde on ice for 15 minutes. Immunohistochemistry was performed using standard methods.

Limb bud culture

Mouse forelimb zeugopod skeletal anlagen were harvested from E12.5 control and *Hox11* mutant *Hoxa11eGFP*-positive embryos. Embryos were harvested in sterile PBS on ice. The ectoderm and soft tissues were carefully mechanically dissected and removed and the zeugopod condensations were collected for culture. Skeletal condensations were rinsed in sterile PBS and transferred to a filter membrane suspended on culture media (above) supplemented with 20nM SAG (Millipore, 566660) or DMSO. After 24 hours, condensations were fixed with 4% paraformaldehyde on ice and whole-mount β-Galactosidase staining was performed. Following imaging, tissue was equilibrated in 30% sucrose overnight and embedded in OCT. Sections were collected at 12μm and imaged.

CHAPTER V

Discussion

Summary of Significant Findings

The most significant finding from this work is the demonstration that Hox11-expressing cells represent a lineage-continuous population of skeletal mesenchymal stem cells throughout the life of the animal. Conflicting data in recent years have led to great debate over the identity and origin of skeletal MSCs. Numerous genetic models have identified populations of cells that enrich, to various extents, for cells with long-term progenitor capacity and multi-lineage contribution to the skeleton, yet the dynamics of the marked populations differ over time depending on the model employed [121, 132, 137, 140-142]. The prevailing theory prior to this work postulated that embryonic progenitors are replaced by long-lived adult MSCs that arise from postnatal stages [118, 128]. Our work is not consistent with this model and provides clear data supporting a developmental origin for life-long skeletal MSCs. Using a *Hoxa11-CreER^{T2}* allele, we demonstrate that skeletal MSCs arise from Hox-expressing stromal cells in the perichondrium at early stages of embryonic skeletal development and persist throughout the lifetime of the animal. These skeletal MSCs contribute to all skeletal mesenchymal lineages including chondrocytes, osteoblasts, and adipocytes, and importantly, contribution to all of these cell types is continuous even through aged adult stages. Finally, using a combination of *Hoxa11eGFP* to identify 'real-time' Hox11-expressing cells and *Hoxa11-CreER^{T2}* to mark *Hox11*-lineage cells, we provide *in vivo* evidence that Hox-positive MSCs are capable of self-renewal throughout life. At all stages examined, the *Hoxa11-CreER^{T2}* marked population behaves as a multi-potent skeletal MSC. Collectively these data define Hox11-positive cells as a life-long skeletal stem cell population.

These data highlight several previously unappreciated characteristics of skeletal MSCs. With our new *Hoxa11-CreER^{T2}* model, we are able to genetically label MSCs in a region specific manner, the zeugopod region of the limb. Thus, this model allows for investigation of MSC migration through space and time in a manner that was previously impossible with existing genetic models. Our data demonstrate that skeletal MSCs arise locally during development and are maintained regionally throughout life. Even following long-term chasing from embryonic to aged adult stages, contribution of *Hoxa11* lineage-marked cells to the skeleton is confined to the zeugopod and no contribution is observed in the stylopod. Reports of blood-borne stromal cells with osteogenic capacity have suggested the existence of a circulating MSC fraction that contributes to bone, particularly following injury repair [218-221]. However, the contribution of blood-borne isolated progenitors to bone has only been investigated *in vitro* or through transplantation studies leaving doubt as to the relevance of these cells in the physiological context. The regional restriction of *Hoxa11-CreER^{T2}* lineage-positive cells throughout life strongly argues against a circulating MSC fraction derived from bone marrow. Additionally, prior work has demonstrated that defects in fracture repair in *Hox11* compound mutants are exclusive to the Hox11-expressing region consistent with no relevant contribution from MSCs from other regions of the skeleton [108, 110]. The observation that MSCs do not mobilize through circulation may provide insight into the mechanism behind the inability of MSCs to home back to the bone marrow space. Unlike HSCs which can re-establish within the bone marrow following injection into circulation, there is abundant evidence that MSCs do not possess this capacity [116, 118, 128, 222]. Instead, injected MSCs become trapped and accumulate in other organs such as the lungs. Given our data demonstrating that MSCs remain local and do not enter the circulation, this would be consistent with their lack of homing capacity.

The demonstration that Hox11-expressing cells are a population of skeletal stem cells throughout the life of the animal may change the way *Hox11* mutant and conditional mutant phenotypes are interpreted. *Hox11* loss-of-function mutation causes severe regional defects in skeletal patterning, growth, and injury repair, suggesting that skeletal stem cells themselves have important roles in skeletal patterning and growth beyond classical functions of adult stem cells such as maintaining tissue homeostasis and

participating in injury repair [80, 108, 109]. Interestingly, analysis of complete *Hox11*
mutants at E18.5 demonstrates that Hox is not required for the specification of MSCs in
the zeugopod. Mutant Hoxa11eGFP-positive stromal cells express MSC markers
PDGFRα/CD51 and equivalent numbers of cells are isolated compared to littermate
controls [110]. *In vitro* tri-lineage differentiation demonstrated defective chondrogenic
and osteogenic differentiation of *Hox11* mutant MSCs, consistent with *Hox11* mutant
phenotypes *in vivo*. These data suggest that Hox11 may function to regulate early lineage
commitment to the skeletal lineages.

Future Directions

Hox function in skeletal MSCs

Recent work from the Wellik lab has clearly demonstrated that Hox11 is, not
only, a marker for skeletal MSCs but is also functional within these cells [80, 108-110]. It
is important reiterate that Hox genes are transcription factors and are expected to exert
their function cell autonomously at the level of transcriptional regulation. As mentioned
above, Hox function does not appear to be required for the specification of MSCs within
the skeleton rather Hox appears to have a role in chondrogenic and osteogenic
differentiation [110]. Hox11 is not expressed in differentiated skeletal cell types therefore
Hox may function during early lineage commitment. Other potential functions for Hox
include maintenance of MSC quiescence, promoting self-renewal, and regulating
signaling between MSCs and other cell types. It is curious to note that several other
genetic models demonstrated to identify progenitor-enriched MSCs, particularly at
developmental stages, are driven by promoters of genes involved in important signaling
pathways such as Hedgehog (*Gli1*-CreER, [141]) or BMP (*Gremlin1*-CreER, [142]). The
pattern of Hoxa11eGFP expression strongly suggests overlap between Hox-expressing
MSCs and the populations marked by *Gli1*-CreER and *Gremlin1*-CreER at embryonic
stages and raises the intriguing possibility that Hox may regulate MSC response to
Hedgehog and/or BMP signaling within skeletal stem/progenitor cells. New *Hox11*
genetic tools will be needed to test the function of Hox in skeletal MSCs *in vivo*.

Several new Hox11 alleles have or are being generated to interrogate the mechanistic function of Hox in MSCs throughout life. A *Hoxd11*-conditional has been generated as part of the body of work described in this thesis and is currently undergoing functional validation [Appx Figure 6.2]. With this allele, complete *Hox11* loss-of function mutants can be induced from any stage and within any cell population using Cre and CreER genetic models. To date, the only method available to examine continuing functions for Hox11 after birth has been through the use of *Hox11* conditional mutants where one *Hox11* allele, either *Hoxa11* or *Hoxd11*, remains wild-type [108, 109]. While these experiments have been informative and indicate continuing functions for Hox11 throughout life, important caveats have limited the conclusions that can be drawn.

Perhaps the easiest example to appreciate the drawbacks of this model is the analyses of Hox11 function during fracture repair [108, 110]. The use of *Hox11* compound mutants for study of adult Hox function is hampered by the severity of the postnatal growth defects observed in these mutants [109]. By adult stages, 8-12 weeks of age when fractures are typically performed, *Hox11* compound mutant zeugopod bones are significantly shorter than control animals and the radius exhibits an abnormal anterior bowing morphology [109]. It is impossible to distinguish which defects in fracture repair can be attributed to loss of Hox11 function and which are secondary to the abnormal bone morphology at these stages [108]. With a *Hoxd11*-conditional allele, complete *Hox11* loss of function mutants can be generated from any stage using animals of the following genotype; *Hoxa11$^{-/-}$;Hoxd11$^{fl/fl}$* containing a tamoxifen inducible *CreER* allele, for example the ubiquitously expressed *ROSA-CreER* [Figure 5.1A]. Complete *Hox11* loss of function will be induced through activation of CreER with tamoxifen prior to or at stages during fracture injury repair to dissect the functions of Hox throughout this process [Figure 5.1A]. It is important to note that *Hox11* conditional mutant animals are maintained on a *Hoxa11* null (*Hoxa11-/-*) background, however *Hoxa11* single mutants have a very mild skeletal phenotype [155]. Wild-type and *Hoxa11* single-mutant animals will be used as controls for all experiments. These experiments will inform our understanding of Hox11 function in the skeleton during injury repair, particularly during callus remodeling where the effect of Hox11 loss-of-function is less clear.
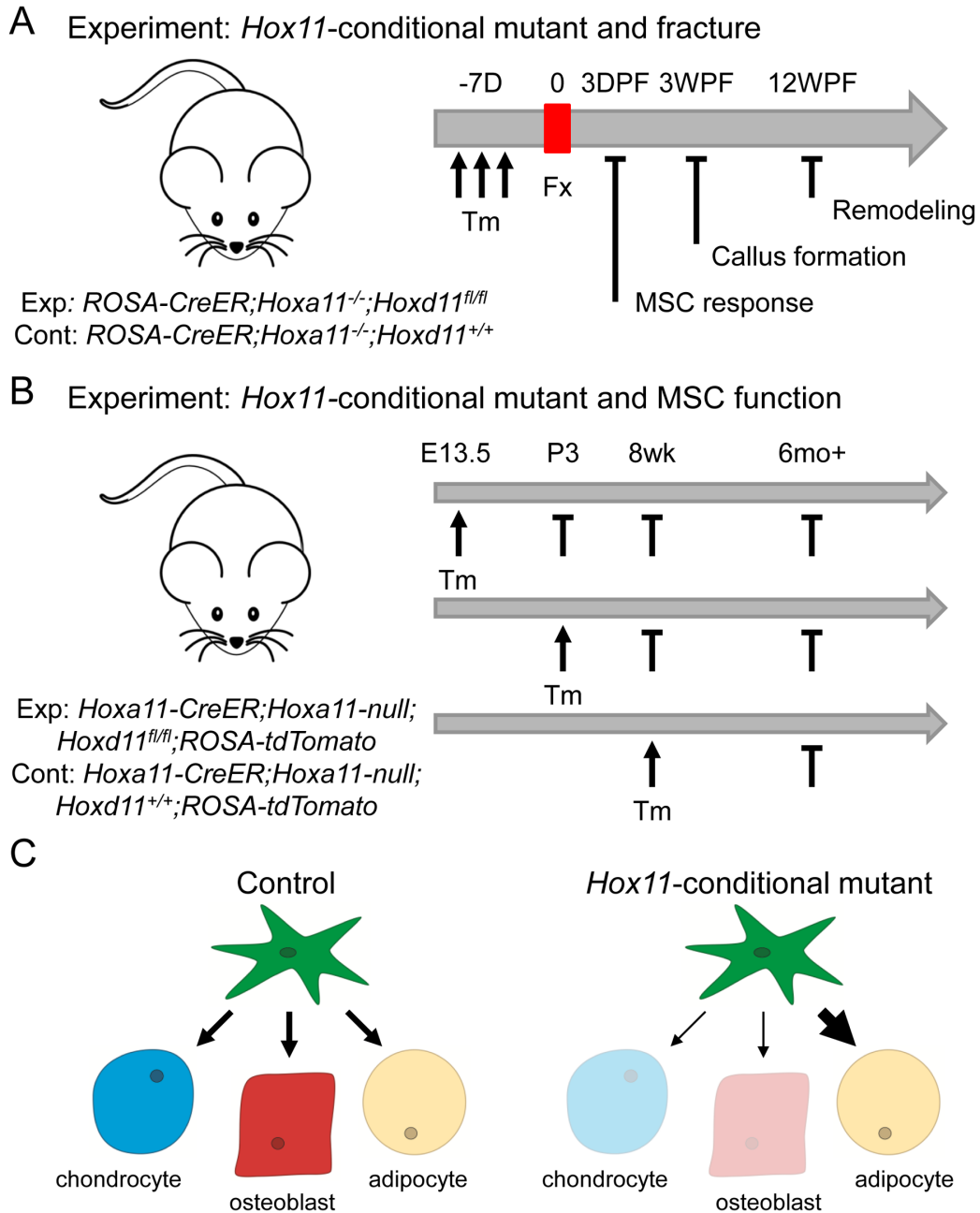
A Experiment: *Hox11*-conditional mutant and fracture

Exp: *ROSA-CreER;Hoxa11⁻/⁻;Hoxd11ᶠˡ/ᶠˡ*
Cont: *ROSA-CreER;Hoxa11⁻/⁻;Hoxd11⁺/⁺*

-7D   0 3DPF 3WPF   12WPF

Tm   Fx

Remodeling
Callus formation
MSC response

B Experiment: *Hox11*-conditional mutant and MSC function

E13.5   P3   8wk   6mo+

Tm

Tm

Tm

Exp: *Hoxa11-CreER;Hoxa11-null;*
Hoxd11ᶠˡ/ᶠˡ;ROSA-tdTomato
Cont: *Hoxa11-CreER;Hoxa11-null;*
Hoxd11⁺/⁺;ROSA-tdTomato

C

Control   *Hox11*-conditional mutant

chondrocyte   osteoblast   adipocyte   chondrocyte   osteoblast   adipocyte

Figure 5.1: Experimental design to test Hox11 function during fracture repair and within skeletal MSCs throughout life. (**A**) Experimental design to test Hox11 function during adult fracture repair. *ROSA-CreER;Hoxa11⁻/⁻;Hoxd11ᶠˡ/ᶠˡ* experimental (Exp) animals and *ROSA-CreER;Hoxa11⁻/⁻;Hoxd11⁺/⁺* control (Cont) animals will be generated by conventional breeding methods. Tamoxifen (Tm) will be administered prior to ulnar fracture (Fx) at 8-10 weeks of age to induce *Hoxd11*-conditional recombination. Mice will be collected for analysis 3 days post fracture (3DPF) to examine the initial MSC response, 3 weeks post fracture (3WPF) to examine osteoblast and chondrocyte formation within the fracture callus, and 12WPF to examine callus remodeling. (**B**) Experimental

design to test Hox function within skeletal MSCs throughout life. *Hoxa11-CreER;Hoxa11-null;Hoxd11$^{fl/fl}$;ROSA-tdTomato* experimental and *Hoxa11-CreER;Hoxa11-null;Hoxd11$^{+/+}$;ROSA-tdTomato* control embryos and mice will be generated by conventional breeding methods. Limiting doses of tamoxifen will be administered at embryonic day 13.5 (E13.5), postnatal day 3 (P3), or 8 weeks of age to induce recombination of *Hoxd11*-conditional allele and expression of *ROSA-tdTomato* reporter allele. Contribution of control and *Hox11* mutant MSCs will be evaluated at relevant time points throughout life as depicted. (**C**) Hox11-expressing MSCs contribute to all three skeletal lineages, chondrocytes, osteoblasts, and adipocytes, throughout life (left). The predicted outcome for *Hox11*-conditional mutant MSCs would be a loss of chondrogenic and osteogenic differentiation and equivalent or increased adipogenic contribution (right).

Conditional *Hox11* mutants can also be used to study the function of Hox within skeletal MSCs throughout life. Using animals of the following genotype; *Hoxa11-CreER/Hoxa11eGFP;Hoxd11^{fl/fl};ROSA-tdTomato*, conditional *Hox11* loss-of-function can be induced in Hox11-expressing MSCs, and contribution *Hox11* mutant MSCs to the skeletal lineages can be measured by tracking tdTomato-positive cells over time [Figure 5.1B]. The advantage of this model is that *Hox11* mutant MSC behavior can be assessed in an otherwise wild-type environment by careful control of the levels of recombination. By modulating the tamoxifen dose to allow sufficient numbers of control MSCs to support normal skeletal function, the impact of *Hox11* loss-of-function on MSC persistence, self-renewal, and multi-lineage contribution can be assessed without disrupting skeletal homeostasis. Given the chondrogenic and osteogenic differentiation defects but normal adipogenic differentiation observed in *Hox11* mutant MSCs *in vitro*, one could predict a loss of chondrogenic and osteogenic contribution and a bias towards adipogenic contribution of conditional mutant MSCs *in vivo* [Figure 5.1C]. Together, these experiments will further define the function of Hox during fracture repair and the roles of Hox11-expressing MSCs throughout life.

Despite decades of study, there continues to be a dearth of understanding of the transcription factor activity of Hox genes particularly with respect to which genes they regulate in different developmental and tissue contexts. All Hox genes contain a homeodomain motif required for DNA binding. The homeodomain structure is highly evolutionarily conserved across species and binds to a core DNA consensus sequence, TAAT or TTAT, that is recognized by nearly all homeodomain containing genes [223-225]. The relatively generic DNA binding properties of the *Hox* genes is difficult to reconcile with the strong genetic evidence for paralog-specific functional domains *in vivo*, referred to as the Hox specificity paradox [226]. Additionally, the conserved structural similarity amongst all Hox genes has raised the question of how Hox specificity is achieved in a context dependent fashion [227]. The activity of DNA-binding Hox co-factors has been demonstrated to modify Hox DNA-binding specificity [228]. For example, most of the Hox4-10 paralogs display comparable cooperative binding with Pbx3 to a *cis*-regulatory region of the *Foxp1* gene, however only Hoxc9 is specifically capable of repressing *Foxp1* expression [229]. Additionally, a recent publication

demonstrated cooperative DNA-binding activity between the hindlimb specific T-box transcription factor, Tbx4, and Hox genes, Hoxc10 and Hoxd13 [230]. Interestingly, while Hoxc10 appears to promote Tbx4 transcriptional activation of target genes, Hoxd13 appears to inhibit Tbx4-mediated transcription. These data demonstrate differential Hox gene function even with cooperation of the same co-factor.

Putative Hox target genes are associated with a diverse array of cellular processes including transcriptional regulation, signal transduction, cell morphology, cell adhesion and migration, the cell cycle, and apoptosis [13, 231-233]. However, for many of these target genes it remains unclear whether Hox proteins directly or indirectly modulate expression. In cultured cancer cell lines, there is significant evidence for Hox gene function in modulating cell-cell and cell-extracellular matrix adhesion [234]. Over-expression and knock-down studies have clearly demonstrated Hox-mediated regulation of several cell adhesion proteins *in vitro* including; integrins and cadherins [234]. Ongoing work has shown a similar requirement for Hox-mediated regulation of cell-cell adhesion in embryogenesis. *Hoxa13* mutants display a marked reduction in *EphrinA7* expression in the embryonic limb bud resulting in reduced cell-cell adhesion and preventing the formation of chondrogenic condensations both *in vivo* and *in vitro* [82]. *EphrinA7* was later shown to be a direct target of both *Hoxa13* and *Hoxd13* [235]. Preliminary microarray analysis from our laboratory comparing *Hox11* control and *Hox11* mutant limb buds at E12.5 demonstrate enrichment for genes related to extracellular matrix and cell adhesion [*data not shown*].

However, apart from a few rare examples, most groups only succeed in identifying a single or small handful of potential targets. In general, the field continues to suffer from a lack genome wide binding information for specific Hox paralogs in tissue relevant contexts inhibiting a global understanding of Hox function. One substantial limitation is availability of rigorously validated antibodies specific for individual Hox proteins. This has prevented the widespread use of chromatin immunoprecipitation (ChIP) assays to identify Hox binding sites within the DNA. Frequently, ChIP data has relied upon either transgenic over-expression of Hox constructs, transfection of tagged Hox constructs into cultured cells or *in vitro* binding assays using purified Hox proteins [235-237]. There are several drawbacks for the use of *in vitro* models for studying

transcription factor binding; perhaps the most important being the loss of the *in vivo* context. Additionally, over-expression can lead to false positives that are not representative of the endogenous state. To this end, ongoing work is being done to generate and validate knock-in FLAG-tagged alleles of *Hoxa11* and *Hoxd11*. These new genetic tools will allow for ChIP experiments to be performed on endogenously expressed Hox constructs. Understanding the gene regulatory functions of Hox on a global scale will have a profound impact on our understanding of how Hox functions to direct development, growth, homeostasis, injury repair, and disease in the skeleton.

Establishment of the bone marrow space and the HSC niche

Our lineage-tracing data demonstrates that Hox11-expressing MSCs in the bone marrow originate from the perichondrial cells in the embryo from at least E13.5. At this stage, the skeletal anlage is completely cartilaginous and *Hoxa11-CreER^{T2}* marked cells will be restricted to the perichondrial tissues surrounding the elements. By adult stages, embryonic *Hoxa11*-lineage cells are found on both the outer surfaces of the bones (perichondrium/periosteum) and within the bones (bone marrow space and endosteal bone surface) demonstrating that the bone marrow fraction of MSCs are lineage-related to cells from the embryonic perichondrium. The mechanism of how the embryonic Hox11-expressing perichondrial stem cells enter and establish the bone marrow MSC compartment is completely unknown.

Formation of the bone marrow space initiates around E15.5 with the invasion of vascular endothelial cells into the hypertrophic zone at the middle of the element [238, 239]. This process occurs about one day after the appearance of Runx2-positive and Osterix-positive pre-osteoblasts on the medial lateral surfaces of the skeletal anlage [240]. As the element grows, osteo-lineage cells are recruited to the developing marrow space, undergo differentiation and mineralize the hypertrophic chondrocyte matrix forming the primary spongiosa [170]. The spongy bone is subsequently remodeled by chondroclasts and osteoclasts to form a hollow tube of cortical bone surrounding the bone marrow cavity [239]. Concurrently, the primary location of hematopoiesis moves from the fetal liver into the bone marrow [241-243]. Current understanding suggests that mesenchymal stromal cells, encompassing skeletal stem cells and other supportive

stromal fibroblasts, are recruited to the bone marrow space by the vasculature [170, 240]. Using an *Osx*-CreER mouse model, Maes *et al*., demonstrated that only osteoblast precursors but not differentiated osteoblasts were capable of invading the bone marrow space during the E14.5 to E16.5 time frame [170]. The intimate association of stromal progenitors and vascular endothelial cells led authors to postulate that stromal cells migrate along the invading endothelial cells to enter the developing bone marrow cavity [170]. The signals that regulate the relocalization of progenitor cells from the perichondrium to the bone marrow space are still being explored.

There are a number of outstanding questions regarding this process. We have demonstrated that Hox11-expressing stromal cells at E14.5 do not overlap with Osx-positive pre-osteoblasts and lineage-tracing data has demonstrated that *Hoxa11*-marked cells more highly enrich for long-term skeletal stem cells than *Osx*-lineage cells. It is unclear whether Hox11-positive MSCs from the outer perichondrial layer will have the same transmigration dynamics as *Osx*-lineage cells. Additionally, how MSC invasion and generation of the HSC niche is coordinated with the transition of HSCs to the bone marrow space is unclear. HSC establishment within the bone marrow occurs during late embryonic and early postnatal stages, however the mechanism of this transition has not been determined. The dogma from adult HSC biology is that HSCs can only maintain their stem cell identity when residing within the HSC niche [244]. If this is true, then it should be impossible for HSCs to travel through the circulation from the liver to the bone marrow during embryonic and fetal stages. This paradox clearly demonstrates that the requirement of HSCs for niche factors during this transition stage is different from adult stages. It is well described that HSC behavior changes during the fetal to adult transition, but the role of the niche stromal cells in these processes is unknown [243]. Careful examination of Hox11eGFP-expressing cell dynamics during the E14.5 to E16.5 temporal window will be needed to determine how and when Hox11-expressing MSCs enter the bone marrow space. Recent studies have suggested that the process of establishing the bone marrow niche during development is similar to the process of vascular regeneration following myeloablation [245]. Knowledge of the relationship between skeletal vascularization, stromal cell recruitment, and establishment of the HSC niche during development of the bone marrow may inform our understanding of bone

marrow recovery following irradiation for bone marrow transplantation. This could have a substantial impact on improving clinical protocols for patients.

Perspective: Hox-expression may identify regional mesenchymal stem/progenitor populations in all musculoskeletal tissues

Regional skeletal MSC populations

The study of bone marrow MSCs is most frequently performed from long bones with analyses of humerus, femur, or tibia bone marrow. Apart from slight differences in proportions of progenitor-enriched MSCs in each bone, as far as has been reported, these progenitors are functionally equivalent. Through our work, we provide compelling evidence that Hox11-expression exclusively defines a regionally restricted MSC population in the zeugopod [[110], Pineault *et al., in submission*]. This observation led us to investigate whether MSCs throughout the body express a region specific Hox profile. We show that Hox expression is exclusive to the LepR-positive MSC compartment of the bone marrow stroma from every bone examined and the regionalized pattern of Hox expression established during development is maintained at adult stages [110]. It is thus far unclear whether the pattern of Hox expression is simply a byproduct of the domains established during development or whether the compliment of Hox genes expressed imparts region-specific regulatory information onto spatially distinct MSC populations. It is important to reiterate that our data demonstrate that Hox11-expressing MSCs are spatially and functionally restricted to the zeugopod at all stages, lending support to the latter hypothesis [[110], Pineault *et al,. in submission*].

One of the biggest outstanding questions in skeletal biology is an understanding of how regional skeletal morphology is established and maintained throughout life. It is remarkable that information regarding regional identity is preserved to adult stages allowing bone to regenerate back to its original form following injury. Genetic evidence supports that Hox genes contain this patterning information and may impart regional specificity to skeletal MSCs. The collective data are consistent with a model whereby Hox-expression defines spatially unique MSC populations during early embryonic development which function to direct region specific skeletal development, growth,

homeostasis and injury repair. Future experiments to define regional Hox function in MSCs throughout the body could have profound consequences on the optimal use of MSCs in various clinical applications and tissue engineering based therapies.

Hox-expressing muscle stromal cells

One remarkable and surprising result from our *Hoxa11-CreER*^{T2} lineage-tracing experiments was the significant lineage contribution of marked cells to mature skeletal muscle fibers. This result was particularly unexpected as Hoxa11eGFP is never expressed in skeletal muscle at any time point examined. Rather, Hoxa11eGFP-expression is restricted to the muscle connective tissue during development and continues to be excluded from mature muscle fibers through postnatal and adult stages [80, 109, 110]. Additionally, Hox11-positive stromal cells and skeletal muscle are derived from two different mesenchymal lineages during development; Hox11-positive cells derive from the lateral plate mesoderm of the limb bud while skeletal muscle cells arise from the somites [46-51, 246]. Myoblasts proliferate and differentiate into mature myofibers within the limb, however the entirely of muscle patterning is established by the tendons and the muscle connective tissue fibroblasts [57, 61, 62, 65]. Loss of *Hox11* function results in regional muscle patterning defects during embryonic stages and further highlights the critical roles these genes play in muscle development.

Skeletal muscle has a remarkable capacity for regeneration. Following injury, muscle stem cells, termed satellite cells, undergo rapid proliferation and differentiation into new myofibers and also self-renew to maintain the stem cell pool [247]. These cells were initially identified by their position within adult skeletal muscle located beneath the basement membrane and adjacent to the myofibrils [248]. Satellite cells express the transcription factor Pax7 and both genetic lineage-tracing studies and transplantation models established the ability of these cells to give rise to regenerating myofibers *in vivo* [247, 249-252]. Genetic ablation of Pax7-positive satellite cells using *Pax7*-CreER^{T2} and a conditional dipthera toxin cassette (*R26R-DTA*) results in complete failure of muscle regeneration confirming that satellite cells are necessary for muscle repair [253-255]. The dogma of satellite cells being the muscle stem cell has been challenged recently by the demonstration that genetic ablation of satellite cells did not accelerate muscle sarcopenia

with age suggesting that while satellite cells are required for muscle regeneration, they may not contribute to muscle homeostasis [256-258]. Furthermore, populations of non-satellite mesenchymal cells have been identified with the capacity to generate differentiated myofibers including mesoangioblasts and PW1+/Pax7- interstitial cells (PICs) [259, 260].

Muscle connective tissue fibroblasts have been the subject of increased study in recent years. In general, two distinct functions have been attributed to these cells. The first function is to support muscle function and regeneration in a non-myogenic capacity. These supportive muscle interstitial cells can be identified by expression of stromal cell markers PDGFRα, CD34, Sca1, and Tcf4 and appear to act as a source of pro-differentiation signals for myoblasts during regeneration [66, 261, 262]. Due to their ability to differentiate into myofibroblasts and adipose cells this population was termed fibro-adipogenic progenitors (FAPs) [261, 262]. Following muscle injury, FAPs proliferate rapidly and in close proximity to satellite cells and function to promote satellite cell differentiation and myofiber formation [66, 261]. Ablation of Tcf4-positive fibroblasts significantly impairs muscle repair resulting in premature satellite cell depletion and smaller regenerated myofibers [66]. These data show that some muscle connective tissue fibroblasts function in an analogous mechanism to muscle connective tissue cells during development to promote muscle fiber organization and fiber type identity during muscle regeneration.

The second general function attributed to muscle connective tissue fibroblasts is actual myogenic contribution to new myofibers, challenging the dogma of the satellite cell as the only muscle stem cell. PW1-positive interstitial cells (PICs) were initially characterized when a muscle-resident, Pax7-negative cell localized to the muscle interstitium was identified that was capable of myogenic differentiation *in vitro* and contributed to new myofibers *in vivo* following injury [260]. PICs and satellite cells derive from distinct mesenchymal lineages during development, making the myogenic contribution of PICs even more surprising [260]. Twist2 expression has also recently been used to identify a non-satellite cell, mesenchymal population with myogenic potential *in vivo* [263]. However, it is still unclear if this population is distinct from PW1 cells as no enrichment for PW1 was observed by flow cytometry and instead high levels

of Sca1 and PDGFRα were observed. Lineage-tracing experiments using an inducible *Twist2*-CreER model provided the first genetic evidence to demonstrate the contribution of a non-satellite cell mesenchymal to mature muscle fibers at homeostasis *in vivo* [263]. Interestingly, *Twist2*-lineage cells are reported to only contribute to type II muscle fibers, specifically type IIb and type IIx, suggesting that this population may represent a fiber-type specific progenitor in muscle. Myogenic contribution by non-satellite cells is an active area of investigation with many questions remaining including how the identified mesenchymal populations are related and if specific sub-populations have unique functional roles at homeostasis and following injury.

Our preliminary observations show that Hoxa11eGFP expression in adult muscle tissue is strongly expressed in the mesenchymal cells of the muscle interstitium and is completely excluded from Pax7-positive satellite cells. In addition, preliminary *Hoxa11* lineage experiments shows a striking contribution to adult skeletal muscle [Figure 5.2] The similarities to the recently reported *Twist2*-lineage cells suggests Hoxa11 expression may identify a similar or overlapping non-satellite cell mesenchymal cell with myogenic capacity. Future studies are necessary to determine the overlap of Hox11 expressing cells with other previously described non-satellite mesenchymal cells using previously indentified markers including Twist2, PDGFRα, Sca1, PW1, and CD34 [260-264]. It is interesting to note that PDGFRα and Sca1 are also frequently used to identify progenitor-enriched MSCs within the bone marrow [133]. While Hox11-expression defines skeletal MSCs throughout life, it is unclear whether *Hoxa11*-lineage marked muscle stromal cells contain myogenic capacity throughout life or whether this activity is stage dependent. Preliminary observations from *Hoxa11-CreER^{T2}* lineage-tracing experiments shows that
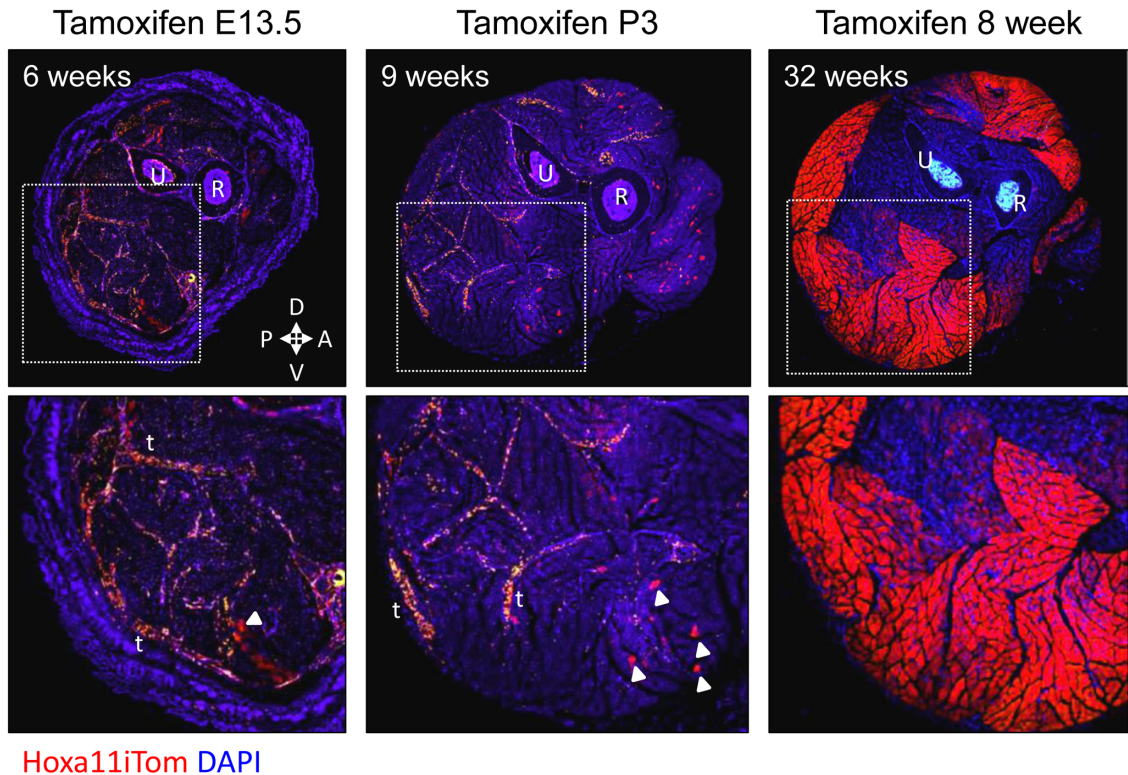
Figure 5.2: *Hoxa11*-**lineage contributes to skeletal muscle robustly from adult stages, contribution is minimal from embryonic and postnatal stages by 8 weeks.** Shown is a low magnification, transverse view of mid-diaphysis adult zeugopod forelimb. All images are oriented with dorsal (D) to the top and anterior (A) to the right. Tamoxifen was administered to *Hoxa11-CreERT2;ROSA-tdTomato* embryos or animals at E13.5, P3, or 8 weeks of age. Lineage contribution to skeletal muscle was examined at the indicated stages. Dotted white line indicates region of high magnification shown below. Arrows indicate rare lineage positive myofibers following lineage tracing from E13.5 or P3. Hoxa11iTom: red, Dapi: blue, t: tendon, R: radius, U: ulna, V: ventral, P: posterior.

the most robust contribution to muscle fibers occurs when induced at early adult stages (8 weeks) and that induction at either embryonic or postnatal stages results in little to no labeling of muscle fibers by 8 weeks of age [Figure 5.2]. However, when chased to aged adult stages (6 months or more) contribution to mature muscle fibers is observed from embryonic, postnatal, and adult stages. More detailed analyses are therefore required to determine the timing of the dynamics of contribution to muscle fibers from each of these stages. It also remains unclear whether *Hoxa11*-lineage cells are fiber type specific myogenic progenitors, similar to *Twist2*-marked cells, or whether they contribute to all myofibers.

Finally, the regional contribution of *Hox11*-lineage cells to the appendicular muscles does not match the functional boundaries of regional Hox11 function established during embryonic development. Muscle patterning defects in *Hox11* mutants are only observed in the zeugopod region of the limb while stylopod muscles are pattered normally [80]. These data are consistent with the functional boundaries for Hox11 function in skeletal patterning [16, 83]. Surprisingly, at adult stages, *Hoxa11*-lineage muscle contribution is not restricted to the skeletal muscles of the zeugopod and instead, lineage contribution is also observed in a small subset of stylopod muscles. It is unclear whether the differences between the boundaries of Hox11 function established during development and the boundaries of lineage contribution are meaningful or are simply reflective of the fact that lineage-labeled stylopod muscles are marked due to their distal insertion sites that reside in the zeugopod region of the limb. Finally, postnatal and adult functions of Hox11 in muscle growth and homeostasis are unknown and represent an exciting avenue for future investigation.

Hox11-lineage contribution to tendon

Tendon stem/progenitor are the least studied of the musculoskeletal MSCs. Tendon is largely considered a non-regenerative tissue; healing occurs very slowly, and generally the original structural and functional characteristics of healthy tendon are never recovered calling into question whether a tendon stem cell even existed [265]. The cellular component of tendon was thought to be exclusively tenocytes and only recently have cells with stem/progenitor capacity been isolated from tendon tissues [266]. The

identified tendon-derived stem cells (TDSCs) exhibit several general characteristics of MSCs including clongenicity, multi-potency, and self-renewal [266]. Similar to the bone marrow MSC field, identification of TDSCs is hampered by the fact that even the best definitions isolate heterogeneous populations of cells of unknown identity and function.

Hox11 expression is observed in all Scx-positive tendon progenitors in the zeugopod during early limb development [80]. As development proceeds, Hoxa11eGFP expression is observed in all progenitor and mature tenocytes and expression in these tissues continues throughout life. *Hoxa11-CreER*^{T2} lineage-tracing data is consistent with these results and shows complete lineage-labeling of all the tendons in the zeugopod at all time points examined. It is important to point out that Hox expression and lineage contribution is observed at the enthesis site and throughout the perichondrium suggesting a common lineage-progenitor for all of these connective tissue compartments. It is highly likely that Hox11 is expressed in TDSCs and *Hoxa11-CreER* may provide a new tool for studying the function of these cells.

Hox-expression as a universal marker of musculoskeletal MSCs

Stromal cells have now been isolated from many mesodermal tissues including; bone/bone marrow, tendon, muscle, adipose, and others [267-269]. Multi-lineage differentiation experiments have coaxed stromal cells from many of these tissues to superficially exhibit chondrogenic, adipogenic, and osteogenic capacity *in vitro*, leading to the poorly supported conclusion that cultures of cells from any connective tissue represent an MSC [116, 270]. From these data the concept of the universal "mesenchymal stem cell" was born [269-272]. This hypothesis postulates that a common progenitor exists for all non-hematopoietic, non-epithelial, mesodermally derived tissues and that this universal progenitor can be isolated from nearly every tissue in the body [118, 129, 267, 269, 273]. Regenerative medicine approaches took this concept further to suggest MSCs were capable of regenerating not only mesodermally derived extra-skeletal tissues but tissues derived from other germ layers such as liver or neurons [274]. The support for this transgerminal plasticity was derived from *in vitro* studies where cultures of neuron-like or liver-like cells were differentiated from poorly defined MSC populations [116]. Evidence for this plasticity *in vivo* has yet to demonstrate clinical

feasibility. The logic for a transgerminal stem cell is not supported by the basic principles of developmental biology, and the concept of the universal mesenchymal stem cell is losing favor as therapeutic success continues to not be realized in clinical trials.

The data presented herein argues against abandoning this concept entirely, at least with respect to musculoskeletal MSCs. Skeletal stem cells, muscle interstitial stromal cells, and tendon-derived stem cells represent developmentally lineage-related stromal populations and a sub-population of these cells are Hox-expressing. Lineage-tracing data argues that all three of these stromal populations originate at least as early as E13.5 during development and persist throughout the life of the animal. Rigorous analysis of Hox-expressing skeletal MSCs strongly support that this population identifies life-long, self-renewing skeletal stem cells. The long-term persistence *Hoxa11*-lineage positive cells within tendon and muscle interstitial cells is consistent with the hypothesis that *Hoxa11*-lineage cells in all musculoskeletal tissues are capable of self-renewal. There is ample evidence that at adult stages, skeletal MSCs, muscle interstitial cells, and TDSCs are no longer equivalent MSC populations however our data demonstrate that they arose from a uniform Hox-expressing mesenchymal population during development.

With the growing library of Hox11 genetic models, tools now exist to dissect how musculoskeletal MSC populations develop and when these populations diverge to become tissue specific stem/progenitors. Isolation of lineage-related stromal cell populations from each of these tissues can be performed on the basis of Hoxa11eGFP expression and exclusion of mature cell types in a way that cannot be accomplished with known flow cytometry markers. Omics profiles of Hoxa11eGFP-positive stromal cells will provide insight into universal properties of MSCs across tissues as well as tissue specific stem/progenitor signatures. These comparisons can also be performed in Hoxa11eGFP-positive cells over time to understand how stem cells are defined and change with age. This knowledge will have a profound impact across many fields deepening our understanding of Hox biology throughout life, improving our understanding of how stem cells develop, and potentially changing how MSCs are used for regenerative and tissue engineering therapies for the musculoskeletal system.

APPENDIX I

Generation of two new *Hox11* alleles via Cas9/CRISPR genetic engineering

Generation of a *Hoxa11-CreER^{T2}* targeted knock-in

Cas9/CRISPR genetic engineering was used to generate a tamoxifen inducible *CreER* knock-in at the *Hoxa11* locus. For our approach, we elected to use two guide RNAs designed to cut near the boundaries of exon 1 of *Hoxa11* and a recombination plasmid [Appx Figure 6.1A]. The use of two guides allowed us to use a 'remove and replace' strategy eliminating all of exon 1 and a small portion of the intron and replacing it with *CreER* sequence. Additionally, the target guide RNA sequence is eliminated in this strategy and is not be present in the recombination plasmid preventing unwanted targeting of Cas9 to the plasmid or the recombined allele. A recombination plasmid was generated containing a tamoxifen-inducible Cre cassette (*CreER^{T2}*) which includes the rabbit β-globin poly-adenylation sequence flanked by 1.3kb of homology upstream and downstream of exon 1 of *Hoxa11* [172]. This editing strategy results in replacement of exon 1 with *CreER^{T2}* while maintaining the endogenous *Hoxa11* upstream and surrounding sequences.

Founder animals (F0) were initially screened by PCR for insertion of *CreER^{T2}* sequence [Appx Figure 6.1B]. Four animals were positive for CreER sequence. Correct targeting to the *Hoxa11* locus was validated by Southern Blot analyses using 5' and 3' flanking probes as well as an internal probe [Appx Figure 6.1C]. Of the four potential founders, three animals were correctly targeted to the Hoxa11 locus, and animal number 27 displayed germline transmission of the allele [Appx Figure 6.1C]. To test for non-specific CreER activity, *Hoxa11-CreER^{T2}* mice were crossed to *ROSA26-LSL-tdTomato*

reporter mice. At 8 weeks of age, no tdTomato expression was observed in the absence of tamoxifen administration [Appx Figure 6.1D].

Two step generation of a *Hoxd11*-conditional allele

Cas9/CRISPR genetic engineering was used to generate a *Hoxd11*-conditional allele with LoxP sequence flanking exon 2 of *Hoxd11* using a two step generation approach. Guide RNAs were targeted to the *Hoxd11* intron and the 3' region downstream of exon 2 and replacement oligos containing 60bp of homologous sequence flanking LoxP sequence were designed [Appx Figure 6.2A]. We elected to use a two step approach for our strategy given prior experience generating a *Hoxa5*-conditional allele. From previous experience generating a *Hoxa5*-conditional allele, if both LoxP sites are targeted simultaneously with the use of two sgRNAs, the most common outcome is deletion of the entire sequence between the sgRNA sites instead of two independent recombination events [Hrycaj, S.M. and Cebrian, C. unpublished results]. Therefore, we elected to use a two-step approach to target the intron LoxP site first and then target the 3' LoxP site [Appx Figure 6.2A].

Following targeting of the intron LoxP site, three animals were sequence verified to contain a correctly targeted LoxP allele [Appx Figure 6.2B]. Male heterozygous pups were used as stud males to generate zygotes for targeting the 3' LoxP site. Following targeting of the 3' LoxP site, six animals were heterozygous for the intron LoxP site and sequence verified to contain a correctly targeted 3' LoxP allele [Appx Figure 6.2C]. Founders were mated to wild-type mice and genotyping of F1 pups was used to determine if both LoxP sites were correctly targeted in *cis* on the same chromosome or targeted in *trans* on two different chromosomes. Animal number 743 was homozygously targeted for the 3' LoxP site and, therefore, most efficiently generated heterozygous pups containing the correctly targeted *Hoxd11*-conditional allele.

To test for LoxP site recombination, the *Hoxd11*-conditional allele was combined with the tamoxifen inducible, ubiquitously expressed *ROSA-CreER* allele. Following tamoxifen administration at 8 weeks of age, recombination of the conditional allele was determined by PCR. Four months after tamoxifen administration, efficient recombination of the allele is observed by the absence of the conditional allele PCR product and

presence of the recombined allele PCR product [Appx Figure 6.2A,D]. Non-recombined DNA was observed in one *Hoxd11*-conditional mutant out of five [Appx Figure 2.6D]. Confirmation that the recombined *Hoxd11*-conditional allele truly functions as a null allele is ongoing. Tamoxifen will be administered to pregnant females at E9.5 and E10.5 to induce recombination at the time when Hox11 is first expressed in the developing limb bud, and the phenotype of embryos with the genotype *Hoxa11$^{-/-}$;Hoxd11$^{fl/fl}$;ROSA-CreER* will be examined at birth. If the recombined *Hoxd11*-conditional allele functions as a null allele, we would expect these embryos to recapitulate the *Hox11* mutant (*Hoxa11$^{-/-}$;Hoxd11$^{-/-}$*) phenotype [83].
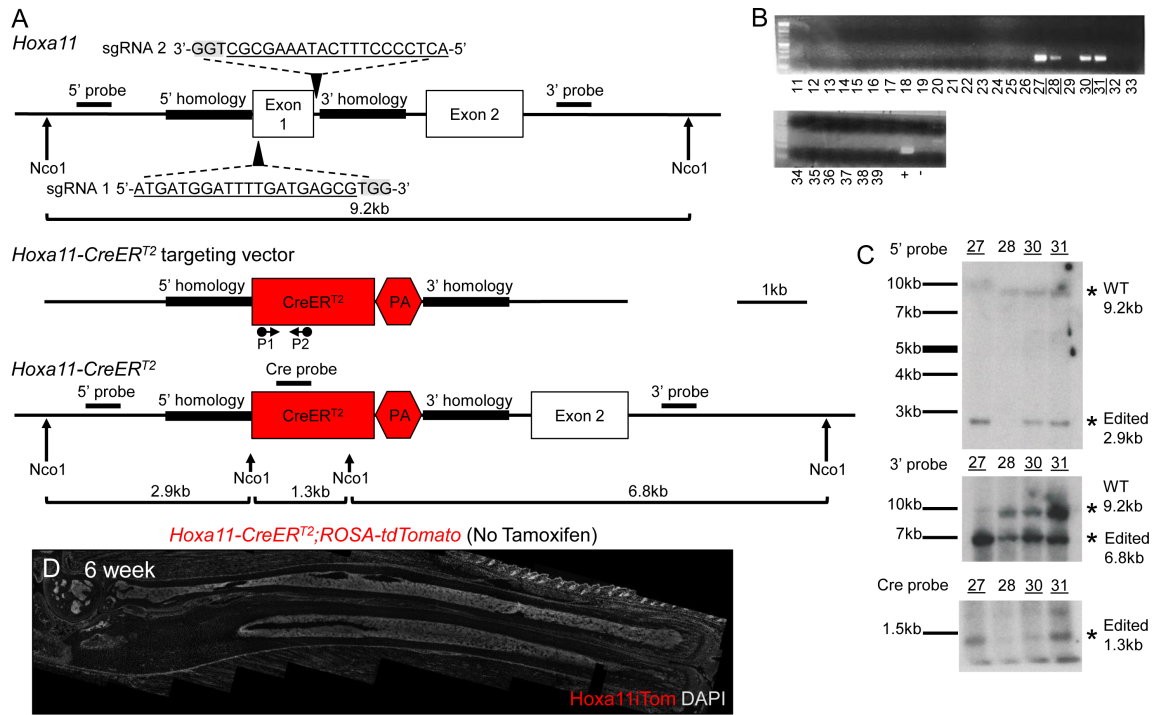
Appendix Figure 6.1: Generation of *Hoxa11-CreER^{T2}* allele via Cas9/CRISPR genetic engineering. (**A**) Schematic of Cas9/CRISPR targeting of *Hoxa11* locus for generation of *Hoxa11-CreER^{T2}* allele. Top: *Hoxa11* locus, positions and sequence of sgRNAs (grey box: PAM), Nco1 restriction sites, positions for 5' and 3' Southern Blot probes and size of wild-type (WT) fragment generated. Middle: *Hoxa11-CreER^{T2}* targeting vector, 5' and 3' homology regions (thick black line), CreER^{T2} and rabbit globin poly-adenylation (PA) insertion (red), and location of Cre PCR primers. Bottom: *Hoxa11-CreER^{T2}* allele, Nco1 restriction sites, positions for 5', 3' and Cre Southern Blot probes and size of edited fragments generated. (**B**) PCR analysis for Cre sequence on 29 live births. (**C**) Southern Blot on four Cre-positive animals using 5' probe (top), 3' probe (middle) and Cre probe (bottom). Wild-type and edited bands and sizes as marked. (**D**) *CreER^{T2}* recombination in the absence of tamoxifen in *Hoxa11-CreER^{T2};ROSA-tdTomato* mice at 6 weeks of age. Fluorescent image - red: *Hoxa11* lineage-marked cells (Hoxa11iTom), grey: DAPI. Repeat of Supplemental Figure 3.2

A

Hoxd11

Exon 1   Intron LoxP   Exon 2   3' LoxP
          oligo 1   oligo 2

sgRNA 1 3'-CCTGTGGGCGCGCTCTTGTCTC-5' sgRNA 2 5'-CCACCCTGCTAAATAAACGCTGG-3'

Hoxd11-conditional

P1 P2   P3 P4

P1   P5   P4
       ◀ 600bp ▶

Hoxd11-conditional: recombined

P1   P4
   ◀ 300bp ▶

B   First round: Intron LoxP

376 377 378   381   386 387   394   389 390

F1 pups from animals 377, 387,
394 used as stud males for
second round of targeting

C   Second round: 3' LoxP

Intron LoxP

742 743 745   750 751 754   761 763   767 770 772

3' LoxP

742 743 745   750 751 754   761   763   767 770 772

743 – Final Founder
750, 767 – Allele in *cis*
742, 745 – Chimeric
763 – LoxP sites in *trans*

D   Primers 1, 4, and 5   Primers 1 and 5

500bp
300bp

1 2 3 4 5 6 7   1 2 3 4 5 6 7

1. *Hox11*-conditional mutant
2. *Hox11*-conditional mutant
3. *Hox11*-conditional mutant
4. *Hox11*-conditional mutant
5. *Hox11*-conditional mutant
6. Control
7. Control

Appendix Figure 6.2: Generation of *Hoxd11*-conditional allele via Cas9/CRISPR genetic engineering. (**A**) Schematic of Cas9/CRISPR targeting of *Hoxd11* locus for generation of *Hoxd11*-conditional allele. Top: *Hoxd11* locus, positions and sequence of sgRNAs (grey boxL PAM), positions of single strand DNA oligos containing 60bp homology sequence flanking LoxP. Middle: targeted *Hoxd11*-conditional allele, position of genotyping primers (red arrows) for the LoxP sites (primers 1-4), position of primers to measure recombination (primers 1,4, and 5). Bottom: recombined *Hoxd11* allele, position of primers to measure recombination (primers 1 and 4). (**B**) PCR genotyping (primers 1 and 2) of F0 animals for recombination at intron LoxP site. Animals 377, 387, and 394 were sequence verified to contain correctly targeted allele, male F1 pups used as

stud males for targeting 3' LoxP site. (**C**) PCR genotyping of F0 animals for intron LoxP site (primers 1 and 2, top) and for recombination at 3' LoxP site (primers 3 and 4, lower). Animals 744, 743, 745, 750, 763, 767 were heterozygous for intron LoxP site and sequence verified to be correctly targeted at 3' LoxP site. Animal 743 contained both LoxP sites in *cis* and was used as the founder animal to generate the *Hoxd11* conditional line. (**D**) Adult control (*ROSA-CreER;Hoxd11$^{+/+}$*) and *Hoxd11*-conditional (*ROSA-CreER;Hoxd11$^{fl/fl}$*) animals were administered tamoxifen chow for 3 weeks beginning at 8 weeks of age and recombination of the *Hoxd11*-conditional allele within the skeletal tissues was examined following a four month chase by PCR. Genotyping with primers for the control and recombined allele (Primers 1, 4, and 5, left) showed nearly complete recombination in *Hoxd11*-conditional mutant animals. Genotyping with primers for the control allele alone (Primers 1 and 5) show low levels of the non-recombined allele only in animal 1.

Materials and Methods

Production of sgRNAs and Cas9 mRNA

All guide sequences were cloned into the pT7-Guide Vector (Blue Heron Biotech, LLC). For generation of the *Hoxd11*-conditional allele, guide sequences were targeted to regions of low conservation in an effort to avoid disrupting DNA regulatory sequences. The guide sequence and approximate locations of sgRNAs, including the corresponding PAM sequence, are illustrated in Appx Figure 6.1A and Appx Figure 6.2A. MEGAshortscript T7 kit (Life Technologies) was used to generate *in vitro* transcribed sgRNA's from the pT7-Guide Vector and products were subsequently purified using the MEGAclear kit (Life Technologies). Using the pT7-Cas9-Nuclease vector (gift from Dr. Moises Mallo), Cas9 mRNA was *in vitro* transcribed using the mMESSAGE mMACHINE T7 ULTRA kit (Life Technologies) and purified using the MEGAclear kit (Life Technologies).

Production of *Hoxa11-CreER^{T2}* targeting plasmid

Homologous sequence flanking exon 1 of *Hoxa11* were synthesized by Blue Heron Biotech, LLC into the pUCminusMCS vector as a continuous insert separated by sequence containing restriction sites for EcoRI, NotI, and HindIII to allow for sub-cloning of *CreER^{T2}* and rabbit β-globin poly-adenylation signal. The 5' homology arm contained 1.3kb immediately upstream of the endogenous *Hoxa11* start site and 3' homology arm contained 1.3kb of sequence immediately downstream of sgRNA 2 as illustrated in Sup Figure 2A. Sequence for CreERT2 and rabbit β-globin poly(A) signal was sub-cloned from pCAG-CreERT2 vector (gift from Connie Cepko, Addgene plasmid #14797, [172]). Targeting of CreERT2 to *Hoxa11* locus preserves endogenous upstream and downstream sequence and creates a null allele; expressing CreERT2 in place of Hoxa11.

Design of LoxP donor oligos for *Hoxd11*-conditional

Cas9 protein generates a double strand break four nucleotides upstream of the PAM sequence (NGG). LoxP sequence was designed to be inserted at the site of the double strand break, splitting the guide target sequence and thus preventing unwanted digestion of the donor oligos or re-cutting of the endogenous chromosome after

recombination. Donor oligos contained 60bp of flanking homology sequence, the LoxP sequence (bold), and a unique restriction site (EcoRI – intron LoxP or NheI – 3' LoxP, uppercase) for optional use in confirming appropriate targeting. Single stranded DNA oligos were purchased from Integrated DNA Technologies.

Intron LoxP donor oligo sequence:

gttgatgagtgggaacacgagagcctcctgcctttcagggagagggtaagtgatctgccGAATTC**ataacttcgtataat gtatgctatacgaagttat**gcact<u>g</u>gacttaaccccaacctctggctggcgctcagctcggagttgagcagatgctcctg

3' LoxP donor oligo sequence:

tctgattagacttacatcatctctagcatttgaaagcaatttgccaccctgctaaataaGCTAGC**ataacttcgtataatgtat gctatacgaagttat**acgc<u>t</u>ggcactttataaaatatagaacaa agtaaaatatagttatattgtttcgtaaac

Zygote injection

Zygote injections were performed as previously described with minor modifications [182]. C57BL/6 female mice were superovulated and mated with C57Bl/6 male mice and one-cell stage embryos were collected for microinjection. CRISPR reagents were microinjected at the following concentrations: Cas9 mRNA (100ng/µL), each sgRNA (50ng/µL), and targeting plasmid (20ng/µL) or DNA oligo (50ng/µL). Freshly injected eggs were transferred into pseudopregnant females and resulting progeny were initially screened for potential recombination events via PCR.

Confirmation of *Hoxa11-CreER^{T2}* targeting

29 live births were recovered from the microinjections and initial screening for CreER targeting was performed by PCR. Approximate location of all primers indicated in Appx Figure 6.1A.

Primers (shown in 5' to 3' orientation):

Cre Fwd (P1): GGACATGTTCAGGGATCGCCAGGC
Cre Rev (P2): CGACGATGAAGCATGTTTAGCTG

Cre-positive animals by PCR were analyzed by Southern Blotting to confirm targeting using 5' and 3' flanking probes and a Cre internal probe with Nco1 digested DNA. Southern blot probes were generated by PCR and randomly labeled with ^{32}P-dCTP. Approximate locations of probes are illustrated in Appx Figure 6.1A.

5' probe (453 bp)

Forward primer: TTTCGGTTCTCCTAGACGCC
Reverse primer: CACGGCGTTTGCATGAGATT

3' probe (533 bp)

Forward primer: TCTGTAGTGAGCGCCTTTGG
Reverse primer: GAGGTTCCCGAGAGACTCCT

Cre probe (408 bp)

Forward primer: GCATTACCGGTCGATGCAACGAGTGATGAG
Reverse primer: GAGTGAACGAACCTGGTCGAAATCAGTGCG

Two step generation of *Hoxd11*-conditional allele

The *Hoxd11*-conditional allele was generated in two stages, targeting each LoxP site sequentially. The intron LoxP site was targeted first and 20 live births were recovered from the first injection. PCR primers D11 Primer 1 and D11 Primer 2 were used to screen for LoxP insertion within the *Hoxd11* intron. PCR products were cloned for sequencing using the TOPO TA cloning kit (Thermo Fisher, 450071). Animals 377, 387, and 394 were verified to contain correctly targeted LoxP sequence within the intron. F1 LoxP-heterozygous males from these lines were used as stud males for targeting of the 3' LoxP site. From the second round of injections, 40 live-births were recovered and D11 Primer 3 and D11 Primer 4 were used to screen for LoxP insertion within the region downstream (3') to *Hoxd11* exon 2. Animals that were potentially positive for 3' LoxP insertion and heterozygous for the *Hoxd11* intron LoxP site were submitted for sequencing. Animals 742, 743, 745, 750, 763, and 767 were sequence verified to contain both correctly targeted LoxP sites. F0 animals were mated to wild-type animals and genotyping analyses of F1 pups using PCR primers for each LoxP site were used to determine germline transmission of both LoxP sites in *cis* along the chromosome. Animal 763 contained LoxP sites in *trans*, animals 742 and 745 were chimeric at the 3' LoxP site, and animals 743, 750, and 767 displayed correct *cis* targeting. Animal 743 was used as the founder for this new mouse line.

To test for proper recombination of the *Hoxd11*-conditional allele, the allele was bred to homozygosity and mated with the tamoxifen inducible, ubiquitously expressed *ROSA-CreER*. Adult mice (8 weeks) were fed tamoxifen chow for 3 weeks and recombination of the allele was assessed by PCR four months later. A three primer genotyping strategy using primers D11 Primer 1, D11 Primer 4, and D11 Primer 5 was designed to measure the relative levels of the *Hoxd11*-conditional allele and the recombined allele. The elongation step was programmed such that D11 Primer 1 and D11 Primer 4 would only generate a product if recombination of the LoxP sites had occurred.

Primers (shown in 5' to 3' orientation):
D11 Primer 1: ATGAGTGGGAACACGAGAGC
D11 Primer 2: AGGCTGGCACTGAGATAGGA
D11 Primer 3: AAAGCAATTTGCCACCCTGC
D11 Primer 4: ACAGGTAAACCAATGCCCAGA
D11 Primer 5: GGGGTACATCCTGGAGTTCTCA

APPENDIX II

Publications and Manuscripts

Chapter I is based on two review articles; the first is published and titled "Hox Genes and Limb Musculoskeletal Development" [105] and second is in preparation and currently titled "Development, repair, and regeneration of the musculoskeletal system" with authors listed Kyriel M. Pineault, Jane Y. Song, and Deneen M. Wellik.

Chapter II is based on a published manuscript titled "*Hox11* genes regulate postnatal longitudinal bone growth and growth plate proliferation" [109].

Chapter III is based on a manuscript in submission titled "Hox expression defines a continuous, self-renewing skeletal mesenchymal stem cell (MSC) population" with authors listed Kyriel M. Pineault, Jane Y. Song, Kenneth M. Kozloff, Daniel Lucas, and Deneen M. Wellik.

REFERENCES

1.	Bateson, W., *Materials for the Study of Variation*. 1894: Macmillan.
2.	Bridges, C.B. and T.H. Morgan, *Third-chromosome group of mutant characters of Drosophila melanogaster*. 1923: Carnegie Institution Of Washington: Washington.
3.	Kaufman, T.C., R. Lewis, and B. Wakimoto, *Cytogenetic Analysis of Chromosome 3 in DROSOPHILA MELANOGASTER: The Homoeotic Gene Complex in Polytene Chromosome Interval 84a-B.* Genetics, 1980. **94**(1): p. 115-33.
4.	Kaufman, T.C., M.A. Seeger, and G. Olsen, *Molecular and genetic organization of the antennapedia gene complex of Drosophila melanogaster.* Adv Genet, 1990. **27**: p. 309-62.
5.	Lewis, E.B., *A gene complex controlling segmentation in Drosophila.* Nature, 1978. **276**(5688): p. 565-70.
6.	Garcia-Fernandez, J., *The genesis and evolution of homeobox gene clusters.* Nat Rev Genet, 2005. **6**(12): p. 881-92.
7.	Duboule, D., *The rise and fall of Hox gene clusters.* Development, 2007. **134**(14): p. 2549-60.
8.	Hurley, I., M.E. Hale, and V.E. Prince, *Duplication events and the evolution of segmental identity.* Evol Dev, 2005. **7**(6): p. 556-67.
9.	Moghadam, H.K., M.M. Ferguson, and R.G. Danzmann, *Evidence for Hox gene duplication in rainbow trout (Oncorhynchus mykiss): a tetraploid model species.* J Mol Evol, 2005. **61**(6): p. 804-18.
10.	Woltering, J.M. and A.J. Durston, *The zebrafish hoxDb cluster has been reduced to a single microRNA.* Nature genetics, 2006. **38**(6): p. 601.
11.	Krumlauf, R., *Hox genes in vertebrate development.* Cell, 1994. **78**(2): p. 191-201.
12.	Scott, M.P., *Vertebrate homeobox gene nomenclature.* Cell, 1992. **71**(4): p. 551-3.
13.	Pearson, J.C., D. Lemons, and W. McGinnis, *Modulating Hox gene functions during animal body patterning.* Nat Rev Genet, 2005. **6**(12): p. 893-904.
14.	Horan, G.S., et al., *Compound mutants for the paralogous hoxa-4, hoxb-4, and hoxd-4 genes show more complete homeotic transformations and a dose-dependent increase in the number of vertebrae transformed.* Genes Dev, 1995. **9**(13): p. 1667-77.
15.	McIntyre, D.C., et al., *Hox patterning of the vertebrate rib cage.* Development, 2007. **134**(16): p. 2981-9.

16.   Wellik, D.M. and M.R. Capecchi, *Hox10 and Hox11 genes are required to globally pattern the mammalian skeleton.* Science, 2003. **301**(5631): p. 363-7.

17.   Chen, F. and M.R. Capecchi, *Targeted mutations in hoxa-9 and hoxb-9 reveal synergistic interactions.* Dev Biol, 1997. **181**(2): p. 186-96.

18.   Chen, F. and M.R. Capecchi, *Paralogous mouse Hox genes, Hoxa9, Hoxb9, and Hoxd9, function together to control development of the mammary gland in response to pregnancy.* Proc Natl Acad Sci U S A, 1999. **96**(2): p. 541-6.

19.   Chen, F., J. Greer, and M.R. Capecchi, *Analysis of Hoxa7/Hoxb7 mutants suggests periodicity in the generation of the different sets of vertebrae.* Mech Dev, 1998. **77**(1): p. 49-57.

20.   Condie, B.G. and M.R. Capecchi, *Mice with targeted disruptions in the paralogous genes hoxa-3 and hoxd-3 reveal synergistic interactions.* Nature, 1994. **370**(6487): p. 304-7.

21.   Davis, A.P., et al., *Absence of radius and ulna in mice lacking hoxa-11 and hoxd-11.* Nature, 1995. **375**(6534): p. 791-5.

22.   Fromental-Ramain, C., et al., *Specific and redundant functions of the paralogous Hoxa-9 and Hoxd-9 genes in forelimb and axial skeleton patterning.* Development, 1996. **122**(2): p. 461-72.

23.   Fromental-Ramain, C., et al., *Hoxa-13 and Hoxd-13 play a crucial role in the patterning of the limb autopod.* Development, 1996. **122**(10): p. 2997-3011.

24.   Manley, N.R. and M.R. Capecchi, *Hox group 3 paralogs regulate the development and migration of the thymus, thyroid, and parathyroid glands.* Dev Biol, 1998. **195**(1): p. 1-15.

25.   Studer, M., et al., *Genetic interactions between Hoxa1 and Hoxb1 reveal new roles in regulation of early hindbrain patterning.* Development, 1998. **125**(6): p. 1025-36.

26.   van den Akker, E., et al., *Axial skeletal patterning in mice lacking all paralogous group 8 Hox genes.* Development, 2001. **128**(10): p. 1911-21.

27.   Wahba, G.M., S.L. Hostikka, and E.M. Carpenter, *The paralogous Hox genes Hoxa10 and Hoxd10 interact to pattern the mouse hindlimb peripheral nervous system and skeleton.* Dev Biol, 2001. **231**(1): p. 87-102.

28.   Wellik, D.M., P.J. Hawkes, and M.R. Capecchi, *Hox11 paralogous genes are essential for metanephric kidney induction.* Genes Dev, 2002. **16**(11): p. 1423-32.

29.   Gavalas, A., et al., *Synergy between Hoxa1 and Hoxb1: the relationship between arch patterning and the generation of cranial neural crest.* Development, 2001. **128**(15): p. 3017-27.

30.   Deschamps, J. and J. van Nes, *Developmental regulation of the Hox genes during axial morphogenesis in the mouse.* Development, 2005. **132**(13): p. 2931-42.

31.   Dressler, G.R. and P. Gruss, *Anterior boundaries of Hox gene expression in mesoderm-derived structures correlate with the linear gene order along the chromosome.* Differentiation, 1989. **41**(3): p. 193-201.

32.   Duboule, D. and P. Dolle, *The structural and functional organization of the murine HOX gene family resembles that of Drosophila homeotic genes.* EMBO J, 1989. **8**(5): p. 1497-505.

33. Gaunt, S.J., *Expression patterns of mouse Hox genes: clues to an understanding of developmental and evolutionary strategies.* Bioessays, 1991. **13**(10): p. 505-13.

34. Gaunt, S.J. and L. Strachan, *Temporal colinearity in expression of anterior Hox genes in developing chick embryos.* Dev Dyn, 1996. **207**(3): p. 270-80.

35. Graham, A., N. Papalopulu, and R. Krumlauf, *The murine and Drosophila homeobox gene complexes have common features of organization and expression.* Cell, 1989. **57**(3): p. 367-78.

36. Iimura, T. and O. Pourquie, *Collinear activation of Hoxb genes during gastrulation is linked to mesoderm cell ingression.* Nature, 2006. **442**(7102): p. 568-71.

37. Izpisua-Belmonte, J., et al., *Murine genes related to the Drosophila AbdB homeotic genes are sequentially expressed during development of the posterior part of the body.* The EMBO Journal, 1991. **10**(8): p. 2279.

38. Duboule, D., *Vertebrate Hox genes and proliferation: an alternative pathway to homeosis?* Current Opinion in Genetics & Development, 1995. **5**(4): p. 525-528.

39. Wellik, D.M., *Hox patterning of the vertebrate axial skeleton.* Dev Dyn, 2007. **236**(9): p. 2454-63.

40. Wellik, D.M., *Hox genes and vertebrate axial pattern.* Curr Top Dev Biol, 2009. **88**: p. 257-78.

41. Mallo, M., T. Vinagre, and M. Carapuco, *The road to the vertebral formula.* Int J Dev Biol, 2009. **53**(8-10): p. 1469-81.

42. Mallo, M., D.M. Wellik, and J. Deschamps, *Hox genes and regional patterning of the vertebrate body plan.* Developmental Biology, 2010. **344**(1): p. 7-15.

43. Carapuço, M., et al., *Hox genes specify vertebral types in the presomitic mesoderm.* Genes & Development, 2005. **19**(18): p. 2116-2121.

44. Hostikka, S.L. and M.R. Capecchi, *The mouse Hoxc11 gene: genomic structure and expression pattern.* Mech Dev, 1998. **70**(1-2): p. 133-45.

45. Kmita, M., et al., *Early developmental arrest of mammalian limbs lacking HoxA/HoxD gene function.* Nature, 2005. **435**(7045): p. 1113-6.

46. Kieny, M. and A. Chevallier, *Autonomy of tendon development in the embryonic chick wing.* J Embryol Exp Morphol, 1979. **49**: p. 153-65.

47. Shellswell, G. and L. Wolpert, *The pattern of muscle and tendon development in the chick wing.* Vertebrate limb and somite morphogenesis, 1977: p. 71-86.

48. Chevallier, A., M. Kieny, and A. Mauger, *Limb-somite relationship: origin of the limb musculature.* Journal of Embryology and Experimental Morphology, 1977. **41**(1): p. 245-258.

49. Christ, B., H.J. Jacob, and M. Jacob, *Experimental analysis of the origin of the wing musculature in avian embryos.* Anat Embryol (Berl), 1977. **150**(2): p. 171-86.

50. Ordahl, C.P. and N.M. Le Douarin, *Two myogenic lineages within the developing somite.* Development, 1992. **114**(2): p. 339-53.

51. Wachtler, F., B. Christ, and H.J. Jacob, *On the determination of mesodermal tissues in the avian embryonic wing bud.* Anat Embryol (Berl), 1981. **161**(3): p. 283-9.

52.   Akiyama, H., et al., *The transcription factor Sox9 has essential roles in successive steps of the chondrocyte differentiation pathway and is required for expression of Sox5 and Sox6.* Genes & development, 2002. **16**(21): p. 2813-2828.

53.   Akiyama, H., et al., *Osteo-chondroprogenitor cells are derived from Sox9 expressing precursors.* Proc Natl Acad Sci U S A, 2005. **102**(41): p. 14665-70.

54.   Bi, W., et al., *Sox9 is required for cartilage formation.* Nature Genetics, 1999. **22**(1): p. 85-89.

55.   Bi, W., et al., *Haploinsufficiency of Sox9 results in defective cartilage primordia and premature skeletal mineralization.* Proc Natl Acad Sci U S A, 2001. **98**(12): p. 6698-703.

56.   Murphy, M. and G. Kardon, *Origin of vertebrate limb muscle: the role of progenitor and myoblast populations.* Curr Top Dev Biol, 2011. **96**: p. 1-32.

57.   Kardon, G., *Muscle and tendon morphogenesis in the avian hind limb.* Development, 1998. **125**(20): p. 4019-32.

58.   Murchison, N.D., et al., *Regulation of tendon differentiation by scleraxis distinguishes force-transmitting tendons from muscle-anchoring tendons.* Development, 2007. **134**(14): p. 2697-708.

59.   Schweitzer, R., et al., *Analysis of the tendon cell fate using Scleraxis, a specific marker for tendons and ligaments.* Development, 2001. **128**(19): p. 3855-66.

60.   Huang, A.H., H.H. Lu, and R. Schweitzer, *Molecular regulation of tendon cell fate during development.* J Orthop Res, 2015. **33**(6): p. 800-12.

61.   Schroeter, S. and K.W. Tosney, *Spatial and temporal patterns of muscle cleavage in the chick thigh and their value as criteria for homology.* Am J Anat, 1991. **191**(4): p. 325-50.

62.   Schroeter, S. and K.W. Tosney, *Ultrastructural and morphometric analysis of the separation of two thigh muscles in the chick.* Am J Anat, 1991. **191**(4): p. 351-68.

63.   Brand-Saberi, B., V. Krenn, and B. Christ, *The control of directed myogenic cell migration in the avian limb bud.* Anatomy and Embryology, 1989. **180**(6): p. 555-566.

64.   Kardon, G., J.K. Campbell, and C.J. Tabin, *Local extrinsic signals determine muscle and endothelial cell fate and patterning in the vertebrate limb.* Dev Cell, 2002. **3**(4): p. 533-45.

65.   Kardon, G., B.D. Harfe, and C.J. Tabin, *A Tcf4-positive mesodermal population provides a prepattern for vertebrate limb muscle patterning.* Dev Cell, 2003. **5**(6): p. 937-44.

66.   Mathew, S.J., et al., *Connective tissue fibroblasts and Tcf4 regulate myogenesis.* Development, 2011. **138**(2): p. 371-84.

67.   Bonnin, M.-A., et al., *Six1 is not involved in limb tendon development, but is expressed in limb connective tissue under Shh regulation.* Mechanisms of development, 2005. **122**(4): p. 573-585.

68.   Havis, E., et al., *TGFbeta and FGF promote tendon progenitor fate and act downstream of muscle contraction to regulate tendon differentiation during chick limb development.* Development, 2016. **143**(20): p. 3839-3851.

69. Huang, A.H., et al., *Musculoskeletal integration at the wrist underlies modular development of limb tendons.* Development, 2015.

70. Benjamin, M. and J.R. Ralphs, *Entheses--the bony attachments of tendons and ligaments.* Ital J Anat Embryol, 2001. **106**(2 Suppl 1): p. 151-7.

71. Galatz, L., et al., *Development of the supraspinatus tendon-to-bone insertion: localized expression of extracellular matrix and growth factor genes.* Journal of Orthopaedic Research, 2007. **25**(12): p. 1621-1628.

72. Thomopoulos, S., et al., *Variation of biomechanical, structural, and compositional properties along the tendon to bone insertion site.* J Orthop Res, 2003. **21**(3): p. 413-9.

73. Zelzer, E., et al., *Tendon-to-bone attachment: from development to maturity.* Birth Defects Res C Embryo Today, 2014. **102**(1): p. 101-12.

74. Schwartz, A.G., F. Long, and S. Thomopoulos, *Enthesis fibrocartilage cells originate from a population of Hedgehog-responsive cells modulated by the loading environment.* Development, 2015. **142**(1): p. 196-206.

75. Breidenbach, A.P., et al., *Ablating hedgehog signaling in tenocytes during development impairs biomechanics and matrix organization of the adult murine patellar tendon enthesis.* J Orthop Res, 2015. **33**(8): p. 1142-51.

76. Standring, S., *Gray's anatomy e-book: the anatomical basis of clinical practice.* 2015: Elsevier Health Sciences.

77. Blitz, E., et al., *Tendon-bone attachment unit is formed modularly by a distinct pool of Scx- and Sox9-positive progenitors.* Development, 2013. **140**(13): p. 2680-90.

78. Sugimoto, Y., et al., *Scx+/Sox9+ progenitors contribute to the establishment of the junction between cartilage and tendon/ligament.* Development, 2013. **140**(11): p. 2280-8.

79. Blitz, E., et al., *Bone ridge patterning during musculoskeletal assembly is mediated through SCX regulation of Bmp4 at the tendon-skeleton junction.* Dev Cell, 2009. **17**(6): p. 861-73.

80. Swinehart, I.T., et al., *Hox11 genes are required for regional patterning and integration of muscle, tendon and bone.* Development, 2013. **140**(22): p. 4574-82.

81. Nelson, L.T., et al., *Generation and expression of a Hoxa11eGFP targeted allele in mice.* Dev Dyn, 2008. **237**(11): p. 3410-6.

82. Stadler, H.S., K.M. Higgins, and M.R. Capecchi, *Loss of Eph-receptor expression correlates with loss of cell adhesion and chondrogenic capacity in Hoxa13 mutant limbs.* Development, 2001. **128**(21): p. 4177-88.

83. Boulet, A.M. and M.R. Capecchi, *Multiple roles of Hoxa11 and Hoxd11 in the formation of the mammalian forelimb zeugopod.* Development, 2004. **131**(2): p. 299-309.

84. Colasanto, M.P., et al., *Development of a subset of forelimb muscles and their attachment sites requires the ulnar-mammary syndrome gene Tbx3.* Disease models & mechanisms, 2016: p. dmm. 025874.

85. Mortlock, D.P. and J.W. Innis, *Mutation of HOXA13 in hand-foot-genital syndrome.* Nat Genet, 1997. **15**(2): p. 179-80.

86.   Utsch, B., et al., *Molecular characterization of HOXA13 polyalanine expansion proteins in hand-foot-genital syndrome.* Am J Med Genet A, 2007. **143A**(24): p. 3161-8.

87.   Tischfield, M.A., et al., *Homozygous HOXA1 mutations disrupt human brainstem, inner ear, cardiovascular and cognitive development.* Nat Genet, 2005. **37**(10): p. 1035-7.

88.   Chang, H.Y., et al., *Diversity, topographic differentiation, and positional memory in human fibroblasts.* Proc Natl Acad Sci U S A, 2002. **99**(20): p. 12877-82.

89.   Rinn, J.L., et al., *Anatomic demarcation by positional variation in fibroblast gene expression programs.* PLoS Genet, 2006. **2**(7): p. e119.

90.   Hrycaj, S.M., et al., *Loss of Hox5 function results in myofibroblast mislocalization and distal lung matrix defects during postnatal development.* Sci China Life Sci, 2018.

91.   Hrycaj, S.M., et al., *Hox5 Genes Regulate the Wnt2/2b-Bmp4-Signaling Axis during Lung Development.* Cell Rep, 2015. **12**(6): p. 903-12.

92.   Giampaolo, A., et al., *HOXB gene expression and function in differentiating purified hematopoietic progenitors.* Stem Cells, 1995. **13 Suppl 1**: p. 90-105.

93.   Giampaolo, A., et al., *Key functional role and lineage-specific expression of selected HOXB genes in purified hematopoietic progenitor differentiation.* Blood, 1994. **84**(11): p. 3637-47.

94.   Kawagoe, H., et al., *Expression of HOX genes, HOX cofactors, and MLL in phenotypically and functionally defined subpopulations of leukemic and normal human hematopoietic cells.* Leukemia, 1999. **13**(5): p. 687-98.

95.   Moretti, P., et al., *Identification of homeobox genes expressed in human haemopoietic progenitor cells.* Gene, 1994. **144**(2): p. 213-9.

96.   Pineault, N., et al., *Differential expression of Hox, Meis1, and Pbx1 genes in primitive cells throughout murine hematopoietic ontogeny.* Exp Hematol, 2002. **30**(1): p. 49-57.

97.   Sauvageau, G., et al., *Differential expression of homeobox genes in functionally distinct CD34+ subpopulations of human bone marrow cells.* Proc Natl Acad Sci U S A, 1994. **91**(25): p. 12223-7.

98.   Shah, N. and S. Sukumar, *The Hox genes and their roles in oncogenesis.* Nat Rev Cancer, 2010. **10**(5): p. 361-71.

99.   Bhatlekar, S., J.Z. Fields, and B.M. Boman, *HOX genes and their role in the development of human cancers.* J Mol Med (Berl), 2014. **92**(8): p. 811-23.

100.   Collins, C.T. and J.L. Hess, *Role of HOXA9 in leukemia: dysregulation, cofactors and essential targets.* Oncogene, 2016. **35**(9): p. 1090-8.

101.   Jerevall, P.L., et al., *Exploring the two-gene ratio in breast cancer--independent roles for HOXB13 and IL17BR in prediction of clinical outcome.* Breast Cancer Res Treat, 2008. **107**(2): p. 225-34.

102.   Ma, X.J., et al., *Gene expression profiles of human breast cancer progression.* Proc Natl Acad Sci U S A, 2003. **100**(10): p. 5974-9.

103.   Jung, C., et al., *HOXB13 homeodomain protein suppresses the growth of prostate cancer cells by the negative regulation of T-cell factor 4.* Cancer Res, 2004. **64**(9): p. 3046-51.

104. Jung, C., et al., *HOXB13 induces growth suppression of prostate cancer cells as a repressor of hormone-activated androgen receptor signaling.* Cancer Res, 2004. **64**(24): p. 9185-92.

105. Pineault, K.M. and D.M. Wellik, *Hox genes and limb musculoskeletal development.* Curr Osteoporos Rep, 2014. **12**(4): p. 420-7.

106. Gersch, R.P., et al., *Reactivation of Hox gene expression during bone regeneration.* J Orthop Res, 2005. **23**(4): p. 882-90.

107. Bais, M., et al., *Transcriptional analysis of fracture healing and the induction of embryonic stem cell-related genes.* PLoS One, 2009. **4**(5): p. e5393.

108. Rux, D.R., et al., *Hox11 Function is Required for Region-Specific Fracture Repair.* Journal of Bone and Mineral Research, 2017: p. n/a-n/a.

109. Pineault, K.M., et al., *Hox11 genes regulate postnatal longitudinal bone growth and growth plate proliferation.* Biol Open, 2015. **4**(11): p. 1538-48.

110. Rux, D.R., et al., *Regionally Restricted Hox Function in Adult Bone Marrow Multipotent Mesenchymal Stem/Stromal Cells.* Developmental Cell, 2016.

111. Friedenstein, A.J., R.K. Chailakhjan, and K.S. Lalykina, *The development of fibroblast colonies in monolayer cultures of guinea-pig bone marrow and spleen cells.* Cell Tissue Kinet, 1970. **3**(4): p. 393-403.

112. Friedenstein, A.J., J.F. Gorskaja, and N.N. Kulagina, *Fibroblast precursors in normal and irradiated mouse hematopoietic organs.* Exp Hematol, 1976. **4**(5): p. 267-74.

113. Friedenstein, A.J., et al., *Marrow microenvironment transfer by heterotopic transplantation of freshly isolated and cultured cells in porous sponges.* Exp Hematol, 1982. **10**(2): p. 217-27.

114. Friedenstein, A.J., et al., *Heterotopic of bone marrow. Analysis of precursor cells for osteogenic and hematopoietic tissues.* Transplantation, 1968. **6**(2): p. 230-47.

115. Owen, M. and A.J. Friedenstein, *Stromal stem cells: marrow-derived osteogenic precursors.* Ciba Found Symp, 1988. **136**: p. 42-60.

116. Bianco, P., et al., *The meaning, the sense and the significance: translating the science of mesenchymal stem cells into medicine.* Nat Med, 2013. **19**(1): p. 35-42.

117. Ono, N. and H. Kronenberg, *Mesenchymal Progenitor Cells for the Osteogenic Lineage.* Current Molecular Biology Reports, 2015: p. 1-6.

118. Kfoury, Y. and David T. Scadden, *Mesenchymal Cell Contributions to the Stem Cell Niche.* Cell Stem Cell, 2015. **16**(3): p. 239-253.

119. Morrison, S.J. and D.T. Scadden, *The bone marrow niche for haematopoietic stem cells.* Nature, 2014. **505**(7483): p. 327-34.

120. Kunisaki, Y., et al., *Arteriolar niches maintain haematopoietic stem cell quiescence.* Nature, 2013. **502**(7473): p. 637-43.

121. Mendez-Ferrer, S., et al., *Mesenchymal and haematopoietic stem cells form a unique bone marrow niche.* Nature, 2010. **466**(7308): p. 829-34.

122. Wilson, A. and A. Trumpp, *Bone-marrow haematopoietic-stem-cell niches.* Nat Rev Immunol, 2006. **6**(2): p. 93-106.

123. Sacchetti, B., et al., *Self-Renewing Osteoprogenitors in Bone Marrow Sinusoids Can Organize a Hematopoietic Microenvironment.* Cell, 2007. **131**(2): p. 324-336.
124. Ding, L. and S.J. Morrison, *Haematopoietic stem cells and early lymphoid progenitors occupy distinct bone marrow niches.* Nature, 2013. **495**(7440): p. 231-5.
125. Ding, L., et al., *Endothelial and perivascular cells maintain haematopoietic stem cells.* Nature, 2012. **481**(7382): p. 457-62.
126. Isern, J., et al., *The neural crest is a source of mesenchymal stem cells with specialized hematopoietic stem cell niche function.* Elife, 2014. **3**: p. e03696.
127. Omatsu, Y., et al., *The Essential Functions of Adipo-osteogenic Progenitors as the Hematopoietic Stem and Progenitor Cell Niche.* Immunity, 2010. **33**(3): p. 387-399.
128. Ono, N. and H.M. Kronenberg, *Bone repair and stem cells.* Current Opinion in Genetics & Development, 2016. **40**: p. 103-107.
129. Chen, K.G., K.R. Johnson, and P.G. Robey, *Mouse Genetic Analysis of Bone Marrow Stem Cell Niches: Technological Pitfalls, Challenges, and Translational Considerations.* Stem Cell Reports, 2017. **9**(5): p. 1343-1358.
130. Ono, N., et al., *Vasculature-Associated Cells Expressing Nestin in Developing Bones Encompass Early Cells in the Osteoblast and Endothelial Lineage.* Developmental Cell, 2014. **29**(3): p. 330-339.
131. Pinho, S., et al., *PDGFRalpha and CD51 mark human nestin+ sphere-forming mesenchymal stem cells capable of hematopoietic progenitor cell expansion.* J Exp Med, 2013. **210**(7): p. 1351-67.
132. Zhou, B.O., et al., *Leptin-Receptor-Expressing Mesenchymal Stromal Cells Represent the Main Source of Bone Formed by Adult Bone Marrow.* Cell Stem Cell, 2014.
133. Morikawa, S., et al., *Prospective identification, isolation, and systemic transplantation of multipotent mesenchymal stem cells in murine bone marrow.* J Exp Med, 2009. **206**(11): p. 2483-96.
134. Ding, L. and S.J. Morrison, *Haematopoietic stem cells and early lymphoid progenitors occupy distinct bone marrow niches.* Nature, 2013. **495**(7440): p. 231-235.
135. Chan, Charles K.F., et al., *Identification and Specification of the Mouse Skeletal Stem Cell.* Cell, 2015. **160**(1–2): p. 285-298.
136. Nusspaumer, G., et al., *Ontogenic Identification and Analysis of Mesenchymal Stromal Cell Populations during Mouse Limb and Long Bone Development.* Stem Cell Reports, 2017. **9**(4): p. 1124-1138.
137. Mizoguchi, T., et al., *Osterix marks distinct waves of primitive and definitive stromal progenitors during bone marrow development.* Dev Cell, 2014. **29**(3): p. 340-9.
138. Greenbaum, A., et al., *CXCL12 in early mesenchymal progenitors is required for haematopoietic stem-cell maintenance.* Nature, 2013. **495**(7440): p. 227-230.
139. Liu, Y., et al., *Osterix-cre labeled progenitor cells contribute to the formation and maintenance of the bone marrow stroma.* PLoS One, 2013. **8**(8): p. e71318.

140. Ono, N., et al., *A subset of chondrogenic cells provides early mesenchymal progenitors in growing bones.* Nat Cell Biol, 2014. **16**(12): p. 1157-1167.
141. Shi, Y., et al., *Gli1 identifies osteogenic progenitors for bone formation and fracture repair.* Nature communications, 2017. **8**(1): p. 2043.
142. Worthley, D.L., et al., *Gremlin 1 identifies a skeletal stem cell with bone, cartilage, and reticular stromal potential.* Cell, 2015. **160**(1): p. 269-284.
143. Mendez-Ferrer, S., D.T. Scadden, and A. Sanchez-Aguilera, *Bone marrow stem cells: current and emerging concepts.* Ann N Y Acad Sci, 2015. **1335**: p. 32-44.
144. Abad, V., et al., *The role of the resting zone in growth plate chondrogenesis.* Endocrinology, 2002. **143**(5): p. 1851-1857.
145. Hunziker, E.B., *Mechanism of longitudinal bone growth and its regulation by growth plate chondrocytes.* Microscopy research and technique, 1994. **28**(6): p. 505-519.
146. Beier, F., *Cell-cycle control and the cartilage growth plate.* Journal of Cellular Physiology, 2005. **202**(1): p. 1-8.
147. Mackie, E.J., L. Tatarczuch, and M. Mirams, *The skeleton: a multi-functional complex organ. The growth plate chondrocyte and endochondral ossification.* Journal of Endocrinology, 2011. **211**(2): p. 109-121.
148. Kronenberg, H.M., *Developmental regulation of the growth plate.* Nature, 2003. **423**(6937): p. 332-336.
149. Wit, J.M. and C. Camacho-Hubner, *Endocrine regulation of longitudinal bone growth.* Endocr Dev, 2011. **21**: p. 30-41.
150. Wilsman, N.J., et al., *Differential growth by growth plates as a function of multiple parameters of chondrocytic kinetics.* Journal of Orthopaedic Research, 1996. **14**(6): p. 927-936.
151. Dollé, P., et al., *Disruption of the Hoxd-13 gene induces localized heterochrony leading to mice with neotenic limbs.* Cell, 1993. **75**(3): p. 431-441.
152. Knosp, W.M., et al., *HOXA13 regulates the expression of bone morphogenetic proteins 2 and 7 to control distal limb morphogenesis.* Development, 2004. **131**(18): p. 4581-4592.
153. Davis, A.P. and M.R. Capecchi, *Axial homeosis and appendicular skeleton defects in mice with a targeted disruption of hoxd-11.* Development, 1994. **120**(8): p. 2187-2198.
154. Favier, B., et al., *Axial skeleton homeosis and forelimb malformations in Hoxd-11 mutant mice.* Proceedings of the National Academy of Sciences, 1995. **92**(1): p. 310-314.
155. Small, K.M. and S.S. Potter, *Homeotic transformations and limb defects in Hox A11 mutant mice.* Genes & development, 1993. **7**(12a): p. 2318-2328.
156. Ballock, R.T. and R.J. O'Keefe, *The Biology of the Growth Plate.* Vol. 85. 2003. 715-726.
157. Farnum, C.E. and N.J. Wilsman, *Determination of proliferative characteristics of growth plate chondrocytes by labeling with bromodeoxyuridine.* Calcif Tissue Int, 1993. **52**(2): p. 110-9.
158. Nilsson, O. and J. Baron, *Fundamental limits on longitudinal bone growth: growth plate senescence and epiphyseal fusion.* Trends in Endocrinology & Metabolism, 2004. **15**(8): p. 370-374.

159. Baron, J., et al., *Catch-up growth after glucocorticoid excess: a mechanism intrinsic to the growth plate.* Endocrinology, 1994. **135**(4): p. 1367-1371.

160. Gafni, R.I. and J. Baron, *Catch-up growth: possible mechanisms.* Pediatric Nephrology, 2000. **14**(7): p. 616-619.

161. Schrier, L., et al., *Depletion of resting zone chondrocytes during growth plate senescence.* Journal of Endocrinology, 2006. **189**(1): p. 27-36.

162. Wilsman, N.J., et al., *Cell cycle analysis of proliferative zone chondrocytes in growth plates elongating at different rates.* Journal of orthopaedic research, 1996. **14**(4): p. 562-572.

163. Schipani, E., et al., *Targeted expression of constitutively active receptors for parathyroid hormone and parathyroid hormone-related peptide delays endochondral bone formation and rescues mice that lack parathyroid hormone-related peptide.* Proceedings of the National Academy of Sciences, 1997. **94**(25): p. 13689-13694.

164. Yallowitz, A.R., et al., *Hox10 genes function in kidney development in the differentiation and integration of the cortical stroma.* PLoS One, 2011. **6**(8): p. 1.

165. Thompson, Z., et al., *A model for intramembranous ossification during fracture healing.* Journal of orthopaedic research, 2002. **20**(5): p. 1091-1098.

166. Schneider, C.A., et al., *671 nih image to imageJ: 25 years of image analysis.* Nature methods, 2012. **9**(7).

167. Smith, L., E.M. Bigelow, and K.J. Jepsen, *Systematic Evaluation of Skeletal Mechanical Function.* Current protocols in mouse biology, 2013: p. 39-67.

168. Logan, M., et al., *Expression of Cre recombinase in the developing mouse limb bud driven by a Prxl enhancer.* genesis, 2002. **33**(2): p. 77-80.

169. Kawanami, A., et al., *Mice expressing GFP and CreER in osteochondro progenitor cells in the periosteum.* Biochemical and Biophysical Research Communications, 2009. **386**(3): p. 477-482.

170. Maes, C., et al., *Osteoblast precursors, but not mature osteoblasts, move into developing and fractured bones along with invading blood vessels.* Dev Cell, 2010. **19**(2): p. 329-44.

171. Siclari, V.A., et al., *Mesenchymal progenitors residing close to the bone surface are functionally distinct from those in the central bone marrow.* Bone, 2013. **53**(2): p. 575-586.

172. Matsuda, T. and C.L. Cepko, *Controlled expression of transgenes introduced by in vivo electroporation.* Proc Natl Acad Sci U S A, 2007. **104**(3): p. 1027-32.

173. Jilka, R.L., *The Relevance of Mouse Models for Investigating Age-Related Bone Loss in Humans.* The Journals of Gerontology: Series A, 2013. **68**(10): p. 1209-1217.

174. Park, D., et al., *Endogenous bone marrow MSCs are dynamic, fate-restricted participants in bone maintenance and regeneration.* Cell Stem Cell, 2012. **10**(3): p. 259-72.

175. Kricun, M.E., *Red-yellow marrow conversion: its effect on the location of some solitary bone lesions.* Skeletal Radiol, 1985. **14**(1): p. 10-9.

176. Chen, G., C. Deng, and Y.P. Li, *TGF-beta and BMP signaling in osteoblast differentiation and bone formation.* Int J Biol Sci, 2012. **8**(2): p. 272-88.

177. Lai, L.P. and J. Mitchell, *Indian hedgehog: its roles and regulation in endochondral bone development.* J Cell Biochem, 2005. **96**(6): p. 1163-73.

178. Yoon, B.S. and K.M. Lyons, *Multiple functions of BMPs in chondrogenesis.* Journal of Cellular Biochemistry, 2004. **93**(1): p. 93-103.

179. Duchamp de Lageneste, O., et al., *Periosteum contains skeletal stem cells with high bone regenerative potential controlled by Periostin.* Nature Communications, 2018. **9**(1): p. 773.

180. DeFalco, J., et al., *Virus-Assisted Mapping of Neural Inputs to a Feeding Center in the Hypothalamus.* Science, 2001. **291**(5513): p. 2608-2613.

181. Madisen, L., et al., *A robust and high-throughput Cre reporting and characterization system for the whole mouse brain.* Nat Neurosci, 2010. **13**(1): p. 133-40.

182. Wu, Y., et al., *Correction of a genetic disease in mouse via use of CRISPR-Cas9.* Cell Stem Cell, 2013. **13**(6): p. 659-62.

183. Kawamoto, T. and M. Shimizu, *A method for preparing 2- to 50-µm-thick fresh-frozen sections of large samples and undecalcified hard tissues.* Histochemistry and Cell Biology, 2000. **113**(5): p. 331-339.

184. Caplan, A., *The cellular and molecular embryology of bone formation.* Bone Miner. Res., 1987. **5**: p. 117-183.

185. Poole, A.R., *The growth plate: cellular physiology, cartilage assembly and mineralization.* Cartilage: molecular aspects, 1991: p. 179-211.

186. Xiong, J., et al., *Matrix-embedded cells control osteoclast formation.* Nat Med, 2011. **17**(10): p. 1235-41.

187. Zakany, J. and D. Duboule, *The role of Hox genes during vertebrate limb development.* Current opinion in genetics & development, 2007. **17**(4): p. 359-366.

188. Karaplis, A.C., et al., *Lethal skeletal dysplasia from targeted disruption of the parathyroid hormone-related peptide gene.* Genes Dev, 1994. **8**(3): p. 277-89.

189. Lanske, B., et al., *PTH/PTHrP receptor in early development and Indian hedgehog-regulated bone growth.* Science, 1996. **273**(5275): p. 663-6.

190. Lee Niswander, T., S. Jeffrey, and G.R. Martin, *A positive feedback loop coordinates growth and patterning in the vertebrate limb.* Nature, 1994. **371**: p. 13.

191. Weir, E.C., et al., *Targeted overexpression of parathyroid hormone-related peptide in chondrocytes causes chondrodysplasia and delayed endochondral bone formation.* Proc Natl Acad Sci U S A, 1996. **93**(19): p. 10240-5.

192. Bitgood, M.J. and A.P. McMahon, *HedgehogandBmpGenes Are Coexpressed at Many Diverse Sites of Cell–Cell Interaction in the Mouse Embryo.* Developmental Biology, 1995. **172**(1): p. 126-138.

193. Koyama, E., et al., *Expression of syndecan-3 and tenascin-C: Possible involvement in periosteum development.* Journal of Orthopaedic Research, 1996. **14**(3): p. 403-412.

194. St-Jacques, B., M. Hammerschmidt, and A.P. McMahon, *Indian hedgehog signaling regulates proliferation and differentiation of chondrocytes and is essential for bone formation.* Genes & development, 1999. **13**(16): p. 2072-2086.

195. Vortkamp, A., et al., *Regulation of rate of cartilage differentiation by Indian hedgehog and PTH-related protein.* Science, 1996. **273**(5275): p. 613-22.
196. Hilton, M.J., et al., *Ihh controls cartilage development by antagonizing Gli3, but requires additional effectors to regulate osteoblast and vascular development.* Development, 2005. **132**(19): p. 4339-4351.
197. Kobayashi, T., et al., *PTHrP and Indian hedgehog control differentiation of growth plate chondrocytes at multiple steps.* Development, 2002. **129**(12): p. 2977-2986.
198. Yoshida, C.A., et al., *Runx2 and Runx3 are essential for chondrocyte maturation, and Runx2 regulates limb growth through induction of Indian hedgehog.* Genes & development, 2004. **18**(8): p. 952-963.
199. Guo, J., et al., *PTH/PTHrP receptor delays chondrocyte hypertrophy via both Runx2-dependent and -independent pathways.* Dev Biol, 2006. **292**(1): p. 116-28.
200. Hinoi, E., et al., *Runx2 inhibits chondrocyte proliferation and hypertrophy through its expression in the perichondrium.* Genes Dev, 2006. **20**(21): p. 2937-42.
201. Yang, Y., et al., *Wnt5a and Wnt5b exhibit distinct activities in coordinating chondrocyte proliferation and differentiation.* Development, 2003. **130**(5): p. 1003-1015.
202. Yamaguchi, T.P., et al., *A Wnt5a pathway underlies outgrowth of multiple structures in the vertebrate embryo.* Development, 1999. **126**(6): p. 1211-1223.
203. Bai, C.B., et al., *Gli2, but not Gli1, is required for initial Shh signaling and ectopic activation of the Shh pathway.* Development, 2002. **129**(20): p. 4753-61.
204. Wilson, C.W. and D.Y. Stainier, *Vertebrate Hedgehog signaling: cilia rule.* BMC Biol, 2010. **8**: p. 102.
205. Frank-Kamenetsky, M., et al., *Small-molecule modulators of Hedgehog signaling: identification and characterization of Smoothened agonists and antagonists.* J Biol, 2002. **1**(2): p. 10.
206. Chen, X., et al., *Initial characterization of PTH-related protein gene-driven lacZ expression in the mouse.* J Bone Miner Res, 2006. **21**(1): p. 113-23.
207. Holtz, A.M., et al., *Secreted HHIP1 interacts with heparan sulfate and regulates Hedgehog ligand localization and function.* The Journal of Cell Biology, 2015. **209**(5): p. 739-758.
208. Koziel, L., et al., *Ext1-Dependent Heparan Sulfate Regulates the Range of Ihh Signaling during Endochondral Ossification.* Developmental Cell, 2004. **6**(6): p. 801-813.
209. Cohen, M.M., *The hedgehog signaling network.* American Journal of Medical Genetics Part A, 2003. **123**(1): p. 5-28.
210. Hung, I.H., et al., *A combined series of Fgf9 and Fgf18 mutant alleles identifies unique and redundant roles in skeletal development.* Developmental Biology.
211. Bai, C.B. and A.L. Joyner, *Gli1 can rescue the in vivo function of Gli2.* Development, 2001. **128**(24): p. 5161-72.

212.   Garcia, A.D., et al., *Sonic hedgehog regulates discrete populations of astrocytes in the adult mouse forebrain.* J Neurosci, 2010. **30**(41): p. 13597-608.

213.   Rigueur, D. and K.M. Lyons, *Whole-mount skeletal staining.* Methods Mol Biol, 2014. **1130**: p. 113-121.

214.   Di Giacomo, G., et al., *Spatio-temporal expression of Pbx3 during mouse organogenesis.* Gene Expr Patterns, 2006. **6**(7): p. 747-57.

215.   Mendelsohn, C., et al., *Stromal cells mediate retinoid-dependent functions essential for renal development.* Development, 1999. **126**(6): p. 1139-48.

216.   Cho, E.A. and G.R. Dressler, *TCF-4 binds beta-catenin and is expressed in distinct regions of the embryonic brain and limbs.* Mech Dev, 1998. **77**(1): p. 9-18.

217.   Larsen, B.M., et al., *Mesenchymal Hox6 function is required for mouse pancreatic endocrine cell differentiation.* Development, 2015. **142**(22): p. 3859-68.

218.   Eghbali-Fatourechi, G.Z., et al., *Circulating osteoblast-lineage cells in humans.* N Engl J Med, 2005. **352**(19): p. 1959-66.

219.   Eghbali-Fatourechi, G.Z., et al., *Characterization of circulating osteoblast lineage cells in humans.* Bone, 2007. **40**(5): p. 1370-7.

220.   Kuznetsov, S.A., et al., *Circulating skeletal stem cells.* J Cell Biol, 2001. **153**(5): p. 1133-40.

221.   Otsuru, S., et al., *Circulating bone marrow-derived osteoblast progenitor cells are recruited to the bone-forming site by the CXCR4/stromal cell-derived factor-1 pathway.* Stem Cells, 2008. **26**(1): p. 223-34.

222.   Hanoun, M. and Paul S. Frenette, *This Niche Is a Maze; An Amazing Niche.* Cell Stem Cell, 2013. **12**(4): p. 391-392.

223.   Berger, M.F., et al., *Variation in homeodomain DNA binding revealed by high-resolution analysis of sequence preferences.* Cell, 2008. **133**(7): p. 1266-76.

224.   Desplan, C., J. Theis, and P.H. O'Farrell, *The sequence specificity of homeodomain-DNA interaction.* Cell, 1988. **54**(7): p. 1081-90.

225.   Noyes, M.B., et al., *Analysis of homeodomain specificities allows the family-wide prediction of preferred recognition sites.* Cell, 2008. **133**(7): p. 1277-89.

226.   Mann, R.S., K.M. Lelli, and R. Joshi, *Hox specificity unique roles for cofactors and collaborators.* Curr Top Dev Biol, 2009. **88**: p. 63-101.

227.   Hayashi, S. and M.P. Scott, *What determines the specificity of action of Drosophila homeodomain proteins?* Cell, 1990. **63**(5): p. 883-894.

228.   Merabet, S. and R.S. Mann, *To Be Specific or Not: The Critical Relationship Between Hox And TALE Proteins.* Trends Genet, 2016. **32**(6): p. 334-347.

229.   Jung, H., et al., *Evolving Hox activity profiles govern diversity in locomotor systems.* Dev Cell, 2014. **29**(2): p. 171-87.

230.   Jain, D., et al., *Regulatory integration of Hox factor activity with T-box factors in limb development.* Development, 2018. **145**(6).

231.   Arderiu, G., et al., *HoxA5 stabilizes adherens junctions via increased Akt1.* Cell Adh Migr, 2007. **1**(4): p. 185-95.

232.   Sanchez-Herrero, E., *Hox targets and cellular functions.* Scientifica (Cairo), 2013. **2013**: p. 738257.

233. Svingen, T. and K. Tonissen, *Hox transcription factors and their elusive mammalian gene targets.* Heredity, 2006. **97**(2): p. 88.
234. Taniguchi, Y., *Hox transcription factors: modulators of cell-cell and cell-extracellular matrix adhesion.* Biomed Res Int, 2014. **2014**: p. 591374.
235. Salsi, V. and V. Zappavigna, *Hoxd13 and Hoxa13 Directly Control the Expression of the EphA7 Ephrin Tyrosine Kinase Receptor in Developing Limbs.* Journal of Biological Chemistry, 2006. **281**(4): p. 1992-1999.
236. Knosp, W.M., et al., *Elucidation, quantitative refinement, and in vivo utilization of the HOXA13 DNA binding site.* J Biol Chem, 2007. **282**(9): p. 6843-53.
237. Lei, H., et al., *The identification of Hoxc8 target genes.* Proc Natl Acad Sci U S A, 2005. **102**(7): p. 2420-4.
238. Karsenty, G. and E.F. Wagner, *Reaching a genetic and molecular understanding of skeletal development.* Dev Cell, 2002. **2**(4): p. 389-406.
239. Kronenberg, H.M., *The role of the perichondrium in fetal bone development.* Ann N Y Acad Sci, 2007. **1116**: p. 59-64.
240. Nakashima, K., et al., *The novel zinc finger-containing transcription factor osterix is required for osteoblast differentiation and bone formation.* Cell, 2002. **108**(1): p. 17-29.
241. Christensen, J.L., et al., *Circulation and chemotaxis of fetal hematopoietic stem cells.* PLoS Biol, 2004. **2**(3): p. E75.
242. Wolber, F.M., et al., *Roles of spleen and liver in development of the murine hematopoietic system.* Exp Hematol, 2002. **30**(9): p. 1010-9.
243. Babovic, S. and C.J. Eaves, *Hierarchical organization of fetal and adult hematopoietic stem cells.* Exp Cell Res, 2014. **329**(2): p. 185-91.
244. Al-Drees, M.A., et al., *Making Blood: The Haematopoietic Niche throughout Ontogeny.* Stem Cells Int, 2015. **2015**: p. 571893.
245. Bowers, E., et al., *Granulocyte-derived TNFalpha promotes vascular and hematopoietic regeneration in the bone marrow.* Nat Med, 2018. **24**(1): p. 95-102.
246. Thorogood, P.V. and J.R. Hinchliffe, *An analysis of the condensation process during chondrogenesis in the embryonic chick hind limb.* Journal of Embryology and Experimental Morphology, 1975. **33**(3): p. 581-606.
247. Collins, C.A. and T.A. Partridge, *Self-renewal of the adult skeletal muscle satellite cell.* Cell Cycle, 2005. **4**(10): p. 1338-41.
248. Mauro, A., *Satellite cell of skeletal muscle fibers.* J Biophys Biochem Cytol, 1961. **9**: p. 493-5.
249. Chen, Y., G. Lin, and J.M. Slack, *Control of muscle regeneration in the Xenopus tadpole tail by Pax7.* Development, 2006. **133**(12): p. 2303-13.
250. Lepper, C. and C.M. Fan, *Inducible lineage tracing of Pax7-descendant cells reveals embryonic origin of adult satellite cells.* Genesis, 2010. **48**(7): p. 424-36.
251. Shea, K.L., et al., *Sprouty1 regulates reversible quiescence of a self-renewing adult muscle stem cell pool during regeneration.* Cell Stem Cell, 2010. **6**(2): p. 117-29.

252. Lepper, C., S.J. Conway, and C.M. Fan, *Adult satellite cells and embryonic muscle progenitors have distinct genetic requirements.* Nature, 2009. **460**(7255): p. 627-31.
253. Lepper, C., T.A. Partridge, and C.M. Fan, *An absolute requirement for Pax7-positive satellite cells in acute injury-induced skeletal muscle regeneration.* Development, 2011. **138**(17): p. 3639-46.
254. Murphy, M.M., et al., *Satellite cells, connective tissue fibroblasts and their interactions are crucial for muscle regeneration.* Development, 2011. **138**(17): p. 3625-37.
255. Sambasivan, R., et al., *Pax7-expressing satellite cells are indispensable for adult skeletal muscle regeneration.* Development, 2011. **138**(17): p. 3647-56.
256. Fry, C.S., et al., *Inducible depletion of satellite cells in adult, sedentary mice impairs muscle regenerative capacity without affecting sarcopenia.* Nat Med, 2015. **21**(1): p. 76-80.
257. Keefe, A.C., et al., *Muscle stem cells contribute to myofibres in sedentary adult mice.* Nat Commun, 2015. **6**: p. 7087.
258. McCarthy, J.J., et al., *Effective fiber hypertrophy in satellite cell-depleted skeletal muscle.* Development, 2011. **138**(17): p. 3657-66.
259. Kuang, S., M.A. Gillespie, and M.A. Rudnicki, *Niche regulation of muscle satellite cell self-renewal and differentiation.* Cell Stem Cell, 2008. **2**(1): p. 22-31.
260. Mitchell, K.J., et al., *Identification and characterization of a non-satellite cell muscle resident progenitor during postnatal development.* Nat Cell Biol, 2010. **12**(3): p. 257-66.
261. Joe, A.W., et al., *Muscle injury activates resident fibro/adipogenic progenitors that facilitate myogenesis.* Nat Cell Biol, 2010. **12**(2): p. 153-63.
262. Uezumi, A., et al., *Mesenchymal progenitors distinct from satellite cells contribute to ectopic fat cell formation in skeletal muscle.* Nat Cell Biol, 2010. **12**(2): p. 143-52.
263. Liu, Y., et al., *Isolation of murine bone marrow derived mesenchymal stem cells using Twist2 Cre transgenic mice.* Bone, 2010. **47**(5): p. 916-925.
264. Minasi, M.G., et al., *The meso-angioblast: a multipotent, self-renewing cell that originates from the dorsal aorta and differentiates into most mesodermal tissues.* Development, 2002. **129**(11): p. 2773-83.
265. Sharma, P. and N. Maffulli, *Biology of tendon injury: healing, modeling and remodeling.* J Musculoskelet Neuronal Interact, 2006. **6**(2): p. 181-90.
266. Bi, Y., et al., *Identification of tendon stem/progenitor cells and the role of the extracellular matrix in their niche.* Nat Med, 2007. **13**(10): p. 1219-27.
267. Klimczak, A. and U. Kozlowska, *Mesenchymal Stromal Cells and Tissue-Specific Progenitor Cells: Their Role in Tissue Homeostasis.* Stem Cells Int, 2016. **2016**: p. 4285215.
268. Meirelles Lda, S. and N.B. Nardi, *Methodology, biology and clinical applications of mesenchymal stem cells.* Front Biosci (Landmark Ed), 2009. **14**: p. 4281-98.
269. Meirelles, L.d.S., P.C. Chagastelles, and N.B. Nardi, *Mesenchymal stem cells reside in virtually all post-natal organs and tissues.* Journal of Cell Science, 2006. **119**(11): p. 2204-2213.

270. Dominici, M., et al., *Minimal criteria for defining multipotent mesenchymal stromal cells. The International Society for Cellular Therapy position statement.* Cytotherapy, 2006. **8**(4): p. 315-317.

271. Caplan, A.I., *Mesenchymal stem cells.* Journal of orthopaedic research, 1991. **9**(5): p. 641-650.

272. Caplan, A.I., *The mesengenic process.* Clinics in plastic surgery, 1994. **21**(3): p. 429-435.

273. Yoshimura, H., et al., *Comparison of rat mesenchymal stem cells derived from bone marrow, synovium, periosteum, adipose tissue, and muscle.* Cell Tissue Res, 2007. **327**(3): p. 449-62.

274. Sanchez-Ramos, J., et al., *Adult bone marrow stromal cells differentiate into neural cells in vitro.* Experimental neurology, 2000. **164**(2): p. 247-256.